Baltic Perspective on Early to early Late Ordovician $\delta^{13}C$ and $\delta^{18}O$ Records and its Paleoenvironmental Significance

Oluwaseun Edward[1,2], Christoph Korte[1], Clemens V. Ullmann[3], Jorge Colmenar[4,5] Nicolas Thibault[1], Gabriella Bagnoli[6], Svend Stouge[4], Christian M. Ø. Rasmussen[4,7]

[1]Department of Geosciences and Natural Resource Management, University of Copenhagen, Øster Voldgade 10, 1350 Copenhagen K, Denmark.
[2]Institute of Earth Surface Dynamics, University of Lausanne, Géopolis, 1015 Lausanne, Switzerland.
[3]Camborne School of Mines, College of Engineering, Mathematics and Physical Sciences, University of Exeter, Penryn Campus, Penryn, Cornwall TR10 9FE, U.K.
[4]Natural History Museum of Denmark, University of Copenhagen, Øster Voldgade 5–7, 1350 Copenhagen K, Denmark.
[5]Instituto Geológico y Minero de España, Ríos Rosas 23, 28040 Madrid, Spain
[6]Department of Earth Sciences, University of Pisa, via St. Maria 53, 56100 Pisa, Italy.
[7]GLOBE Institute, University of Copenhagen, Øster Voldgade 5–7, 1350 Copenhagen K, Denmark.

Corresponding author: Christian M. Ø. Rasmussen (c.macorum@sund.ku.dk)

Key Points:

- New paired Baltic carbonate dataset improves Ordovician ^{18}O- and ^{13}C-record
- The new data supports Middle Ordovician climatic cooling
- Regional/intra-basinal consistency of oxygen isotope trends indicate primary nature of paleoenvironmental changes

Abstract

The current study presents new bed-by-bed brachiopod $\delta^{13}C$ and $\delta^{18}O$ records from Öland, Sweden, which together with previously published data from the East Baltic region, constitutes a high-resolution paired brachiopod and bulk rock carbon and oxygen isotope archive through the Lower to Upper Ordovician of Baltoscandia. This new dataset refines the temporal control on the global Ordovician $\delta^{18}O$-trend considerably, improving paleoenvironmental reconstructions through the main phase of the Great Ordovician Biodiversification Event (GOBE). The new brachiopod carbon and oxygen isotope records from Öland display strong similarity with the East Baltic records, elucidating the regional consistency as well as global correlation utility of the ensuing composite Baltoscandian Early to Middle Ordovician carbon and oxygen isotope record. The carbon isotope record from Öland indicates that prominent carbon cycle perturbations are recorded in both brachiopods and bulk carbonates, most notably the MDICE (Mid-Darriwilian Carbon Isotope Excursion). The oxygen isotope record reveals a long-term Early to Late Ordovician trend of increasingly heavier brachiopod $\delta^{18}O$ values, with a pronounced increase during the Middle Ordovician Darriwilian Age. We interpret this trend as dominantly reflecting a paleotemperature signal indicating progressively cooler Early to Middle Ordovician climate with glacio-eustasy. Our Baltic $\delta^{18}O$ values are therefore consistent with postulations that the biotic radiations during the GOBE and climatic cooling during the Darriwilian were strongly linked.

Plain Language Summary

Oxygen isotope values obtained from fossil brachiopod shells have traditionally been used as a faithful paleoclimatic proxy to shed light on temperature trends in ancient oceans. However, because brachiopod shells are susceptible to diagenetic overprint after burial, secular oxygen isotope trends derived from these fossils are often questioned – notably the farther one goes back in geological time. In this study, we present temporally well-resolved oxygen isotope data from Early–early Late Ordovician rocks of Öland, Sweden. This interval is important in Earth history as it brackets the greatest marine biodiversification event known in the fossil record and coincides with a global climatic cooling phase (determined based on proxies other than oxygen isotopes). The current study therefore provides an excellent test of the spatial and temporal consistency of the secular Ordovician oxygen isotope trend. We find that although our data is probably affected by diagenetic modification, primary paleoclimatic signals are preserved. Furthermore, as current global Ordovician oxygen isotope records lack sufficient resolution because they comprise data from geographically widely distributed low-paleolatitude localities, our new high-resolution dataset tied precisely to conodont biostratigraphy on the bed-by-bed scale from one mid-paleolatitude region, provides significant temporal insights that considerably improves our understanding of the paleoclimatic development during the Ordovician.

1 Introduction

The Ordovician Period was characterized by drastic changes in biodiversity levels and ecosystem engineering (Kröger, Franeck, & Rasmussen, 2019; C. M. Ø. Rasmussen, Kröger, Nielsen, & Colmenar, 2019). Elevated changes in plate movements caused fundamental reorganization of the global paleogeographic configuration as continents rifted off the major continent Gondwana and towards lower latitudes (Cocks & Torsvik, 2005; McKenzie, Hughes, Gill, & Myrow, 2014; Torsvik et al., 2012). This prominent dispersal of continents may have constituted a first-order control on species richness as provincialism increased (Valentine & Moores, 1970; Zaffos, Finnegan, & Peters, 2017) and contributed to significant

changes in global sea level (Hallam, 1992; Haq and Schutter, 2008), which were exacerbated by transient climatic shifts (Barnes, 2004; Finnegan et al., 2011; Fortey & Cocks, 2005; Quinton, Speir, Miller, Ethington, & MacLeod, 2018; C. M. Ø. Rasmussen et al., 2016; M. R. Saltzman & Young, 2005; Trotter, Williams, Barnes, Lécuyer, & Nicoll, 2008; Vandenbroucke et al., 2010). Furthermore, carbon isotope excursions hint at major perturbations to the global carbon cycle at this time (Ainsaar et al., 2010; Bergström, Saltzman, Leslie, Ferretti, & Young, 2015; Lindskog, Eriksson, Bergström, & Young, 2019; M. M. Saltzman & Thomas, 2012; M. R. Saltzman & Young, 2005), further indicating a coupling between Earth system changes and biodiversity trends during the Ordovician, the most important of which was the Great Ordovician Biodiversification Event (GOBE).
Several hypotheses have been put forward regarding potential triggers of the GOBE including environmental perturbations related to asteroid impact on Earth (Schmitz et al., 2019), changes in weathering patterns and nutrient delivery to the oceans due to the Taconic orogeny (Cárdenas & Harries, 2010; Miller & Mao, 1995) and increased ocean-atmosphere oxygenation (Edwards, Saltzman, Royer, & Fike, 2017; Knoll & Carroll, 1999). However, other evidence points to Middle Ordovician climatic cooling and subsequent reduction of physiological stressors on marine organisms as a main driver (Goldberg, Present, Finnegan, & Bergmann, 2021; C. M. Ø. Rasmussen et al., 2016; Trotter et al., 2008). The evidence for long-term Ordovician climate change mainly emanates from oxygen isotope compositions of fossil brachiopods and conodonts, which show a secular trend towards generally heavier values from the Early to Late Ordovician. Although different views have been advanced to explain this trend, such as changing seawater oxygen isotope composition, diagenesis, or climate change (Bergmann et al., 2018; Shields et al., 2003; Trotter et al., 2008; Veizer et al., 1999; Veizer, Godderis, & Francois, 2000; Veizer & Prokoph, 2015), sedimentological, sequence stratigraphical and paleontological data have all supported the notion of shorter-term cooling climate, particularly for the Middle Ordovician interval (Dabard et al., 2015; Ghobadi Pour, Williams, & Popov, 2007; Le Hérissé, Al-Ruwaili, Miller, & Vecoli, 2007; Lindskog & Eriksson, 2017; A. T. Nielsen, 2004; C. M. Ø. Rasmussen, Nielsen, & Harper, 2009; J. A. Rasmussen & Stouge, 2018; Turner, Armstrong, Wilson, & Makhlouf, 2012).
To further test this view during the Early–Middle Ordovician, the current study presents new high-resolution oxygen and carbon isotope data based on fossil brachiopod and bulk carbonate samples from the island of Öland situated in the Baltic Sea (Figure 1). Particularly in the context of the long-term Ordovician oxygen isotope trend, this interval has been somewhat neglected probably due to the much larger perturbations in the $\delta^{18}O$-record during the earlier and later parts of the Ordovician (Shields et al., 2003; Veizer & Prokoph, 2015) (Figure 2). Given that both of these intervals may well have been outside the optimal temperature range for most organisms (either too warm or too cool), even a low amplitude change in temperatures during the Dapingian–Darriwilian global stages could have been significant enough for increasing the carrying capacity of ecosystems.
We test the regional consistency of previously reported Baltoscandian Ordovician oxygen isotope trends, as well as the global correlation potential of current global C and O isotope curves (e.g. Shields et al., 2003; Veizer et al., 1999; Veizer & Prokoph, 2015) which remain based on sporadic sampling in the Ordovician interval. Thus, the current study enables, for the first time, an intra-basinal comparison of fossil brachiopod carbon and oxygen isotope compositions spanning the Early Ordovician (Floian) to Middle Ordovician (Darriwilian) interval. Additionally, material is sampled through to the Late Ordovician (late Sandbian) from Öland, Sweden, complementing the global Ordovician stable isotope record by adding better temporal resolution tied precisely to conodont biostratigraphy.

2 Geological Setting

The paleocontinent of Baltica comprises most of northern Europe and consists of Archaean and Proterozoic rocks forming the East European craton (Cocks & Torsvik, 2005). The Ural Mountains in the East, the Trans-European Suture Zone to the south-west and the Scandinavian Caledonides in the north-west border this paleocontinent. During the earliest Cambrian, Baltica rifted off the continent of Gondwana, which opened the Tornquist Sea to the southwest and separated Gondwana and Baltica. The drifting phase of Baltica was associated with anticlockwise rotation starting in the mid-Cambrian and lasted into the Middle Ordovician (Torsvik & Rehnström, 2003). Baltica moved from high southerly to intermediate latitudes by the Middle Ordovician and continued towards the paleoequator throughout the Ordovician (Cocks & Torsvik, 2005; Torsvik et al., 1992; Torsvik et al., 2012). In this period, the passive margin was influenced by continental thermal submergence and first and second order sea-level rises, which resulted in the generation of an extensive epicontinental platform sea (A. T. Nielsen, 2004; Torsvik & Cocks, 2016). Baltica remained tectonically calm until the late Middle Ordovician and was bounded by the Tornquist Sea to the southwest and the Iapetus Ocean to the northwest. When the microcontinent Avalonia reached Baltica, it first resulted in the development of an extensive hiatus across the platform as well as Avalonian volcanism, which became evident in the Sandbian (early Late Ordovician), during which a complex of bentonites appeared on Baltica as subduction beneath Avalonia commenced (Huff, Bergström, & Kolata, 1992; Torsvik & Rehnström, 2003). This phase likely commenced already during the early Darriwilian as numerous bentonites are found in Scanian shale deposits as well as in contemporaneous carbonate successions in Sweden (Bagnoli & Stouge, 1999; Lindskog, Costa, Rasmussen, Connelly, & Eriksson, 2017). The main feature of the paleocontinent, the Baltoscandian Paleobasin, trends west-southwest (WSW) to east-northeast (ENE). The deposition of the Lower to Middle Ordovician sedimentary successions in the basin took place under shallow to deep epicontinental seawater conditions on the shelf of the stable craton. In this calm period, the sedimentary deposits were extensive and covered the areas of Scandinavia, the east Baltic countries and eastern Russia, Ukraine and northern Poland culminating during the sea-level highstand in the Floian (*evae* transgression; Early Ordovician). Sediment accumulation was slow and mid Cambrian and Lower–Middle Ordovician deposits were condensed, which resulted in the fine clastic and organic-rich Alum Shale Formation that persisted from the Cambrian into the Early Ordovician and the overlying carbonate blanket of the Lower to Middle Ordovician Orthoceratite limestone.

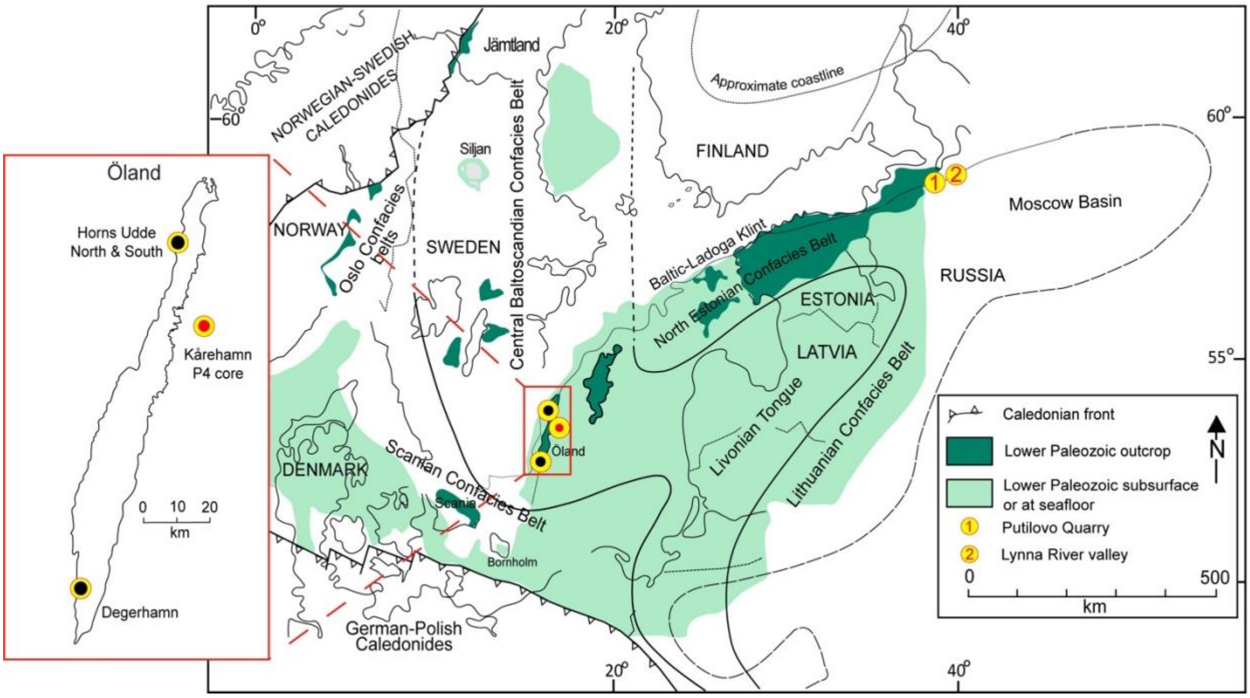

Figure 1: *The confacies belts of the Ordovician Baltoscandian Paleobasin with lower Paleozoic outcrop and subsurface extent shown. Localities discussed in the text are highlighted. Insert map of Öland show an enlarged view of the current study's sampling sites. Modified after Jaanusson (1982a).*

The characteristic lithofacies arrangement of Männil (1966) was combined with the faunal distribution and divided into three broad confacies belts (Jaanusson, 1976, 1982a, 1995) (Figure 1). These belts differ from each other in types of sedimentation, faunal diversity and abundance. Öland experienced little burial, although there is a gradient from thermally immature rocks in the North (CAI: 1) to early mature rocks (CAI: ca. 1.5) in the South (Bergström, 1980; Tullborg, Larsson, Björklund, Stigh, & Samuelsson, 1995).
Due to widespread Ordovician outcrops and well-preserved fossils, a relatively simple tectonic regime with absence of significant thermal alteration, the Baltoscandian Paleobasin in general, and Öland, represents an ideal site for investigating the Early–Middle Ordovician carbon and oxygen isotope record.

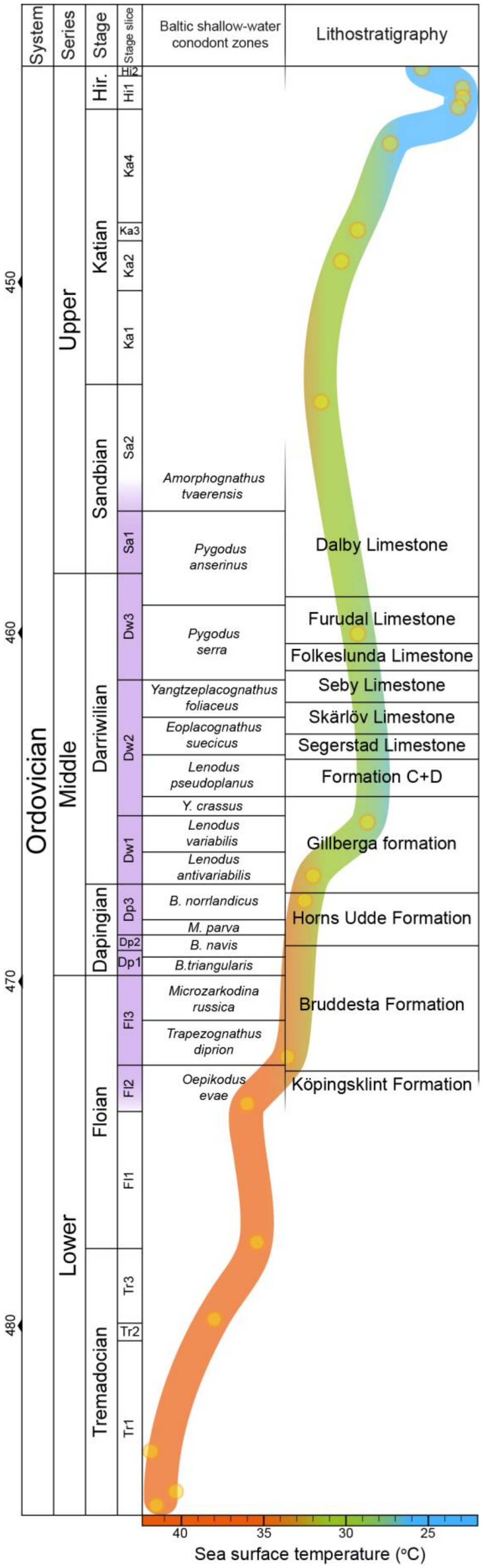

Figure 2: *Ordovician chronostratigraphy and conodont δ^{18}O apatite paleothermometry. The studied interval is highlighted in purple with the litho- and conodont biostratigraphy of northern Öland shown. Numbers on far left are in million years. The oxygen isotope curve is modified from Trotter et al. (2008). Orange colors denote temperatures above present-day tropical sea surface average, green shading present-day window and blue shading below present-day levels. Note that the optimal temperature is reached during the uppermost Dapingian–lowermost Darriwilian Gillberga Formation* on Öland.

3 Lithostratigraphy and biostratigraphy

The Lower to Middle Ordovician (Floian to mid-Darriwilian) Orthoceratite limestone on Öland is composed of green, grey- and red carbonate sedimentary rocks. The limestone is highly condensed, often glauconitic and with low-diversity skeletal composition (Figure 3). Many diastems occur in the succession and these are commonly marked by discontinuity surfaces (Jaanusson, 1961; Lindström, 1979) and less commonly, burrowed and mineralized corrosion hard ground/firm grounds are present (Ekdale & Bromley, 2001). The average carbonate accumulation rate and low siliciclastic input were in the order of 1– 4 mm per 1000 years and sea-level fluctuation was a significant factor for the lithofacies development (Chen & Lindström, 1991; Jaanusson, 1982b; Lindskog et al., 2017; Lindström, 1984; Stouge, 2004). According to the confacies belts of Jaanusson (1976, 1995), the island of Öland lies within the Central Baltoscandia confacies belt, where the northern part is closer to the Estonian confacies belt than the southern part of the island (Figure 1).

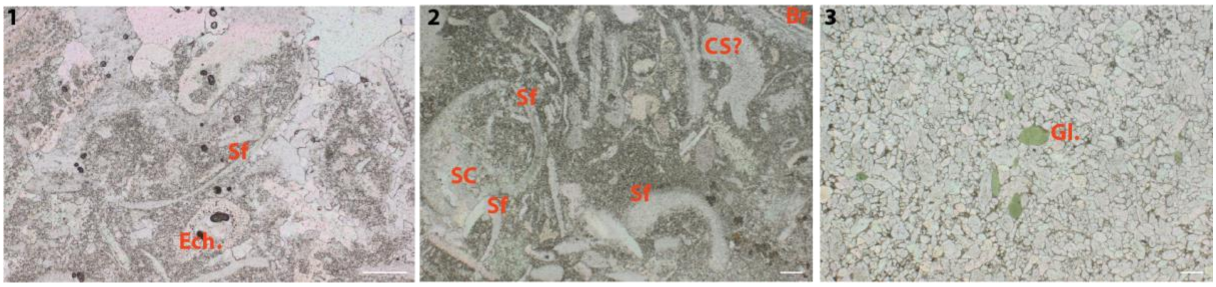

Figure 3: *Photomicrographs showing carbonate microfacies in the study area. Sf = undifferentiated skeletal fragments, Ech. = echinoderm, SC = sparry calcite, CS? = cephalopod shell, Br = brachiopod shell, Gl. = glauconite grain.* ***1.*** *Sample OLK-16, bioclastic packstone, Sandbian.* ***2.*** *Sample OLD-1, bioclastic packstone, Darriwilian.* ***3.*** *Sample OLH-11, glauconitic grainstone, Floian.*

The Öland coastal cliff sections, onshore drill cores and the Kårehamn offshore drill core (Bohlin, 1949, 1953; Stouge, 2004; Wu, Calner, & Lehnert, 2017) are assigned to twelve lithostratigraphic units, although some of them are informal. The entire upper Lower to lower Upper Ordovician succession is further biostratigraphically well constrained based on conodonts. The litho-, bio- and chronostratigraphic schemes used here as reference are shown in Figure 2 and have been compiled based on information from several sources including (Bagnoli & Stouge, 1997; Bergström, 1971, 2007; Bergström, Chen, Gutiérrez-Marco, & Dronov, 2009; Lindström, 1971; Löfgren, 2000, 2003; Stouge, 2004; Stouge & Bagnoli, 1990; Stouge, Bagnoli, & Rasmussen, 2020; van Wamel, 1974; Wu et al., 2017; Zhang, 1998).

3.1 Sampled successions

3.1.1 Horns Udde North section

The Horns Udde North section lies ca. 1.5 km to the northeast of the Cape of Horns Udde (Figure 1). The complete sedimentary succession comprises Cambrian to lower Middle Ordovician (Darriwilian) sedimentary rocks. However, the Cambrian and the lowermost Ordovician (lower Tremadocian) strata in the beach zone are completely covered by rubble. The section has been described in detail by Lindström (1963), Tjernvik (1956), van Wamel (1974) and the most recent conodont zonation has been provided by Bagnoli and Stouge (1997) who sampled the section thoroughly in high resolution (Figure 4). The exposed succession consists of glauconitic siltstone, nodular grey to red mottled limestone, and grey to reddish-brown green mottled limestone with marly interbeds and several discontinuity surfaces. The succession is referred to the Köpingsklint, Bruddesta, Horns Udde and Gillberga formations respectively, with the Lower–Middle Ordovician boundary placed within the Bruddesta Formation (Stouge, 2004; van Wamel, 1974) (Figure 4). Dome-like structures and a pronounced hardground complex known as 'Blommiga bladet' (= Flowery sheet in English; see Figure 4; (Bohlin, 1949; Ekdale & Bromley, 2001) lies within the Bruddesta Formation. Just above the base of the Horns Udde Formation, three distinct horizons, collectively 0.2 m thick, and composed of prominent haematite-impregnated bacterial-like structures occur (named 'Blodläget' = 'Bloody layer' in English; (Bohlin, 1949; Stouge, 2004). The uppermost 2.3m of strata in the section belong to the lower sub-unit of the overlying Gillberga Formation (= Formation A of Stouge (2004)). These beds are composed of unevenly bedded, glauconitic limestone with some intervals of nodular limestone interbedded with minor green glauconite shale.

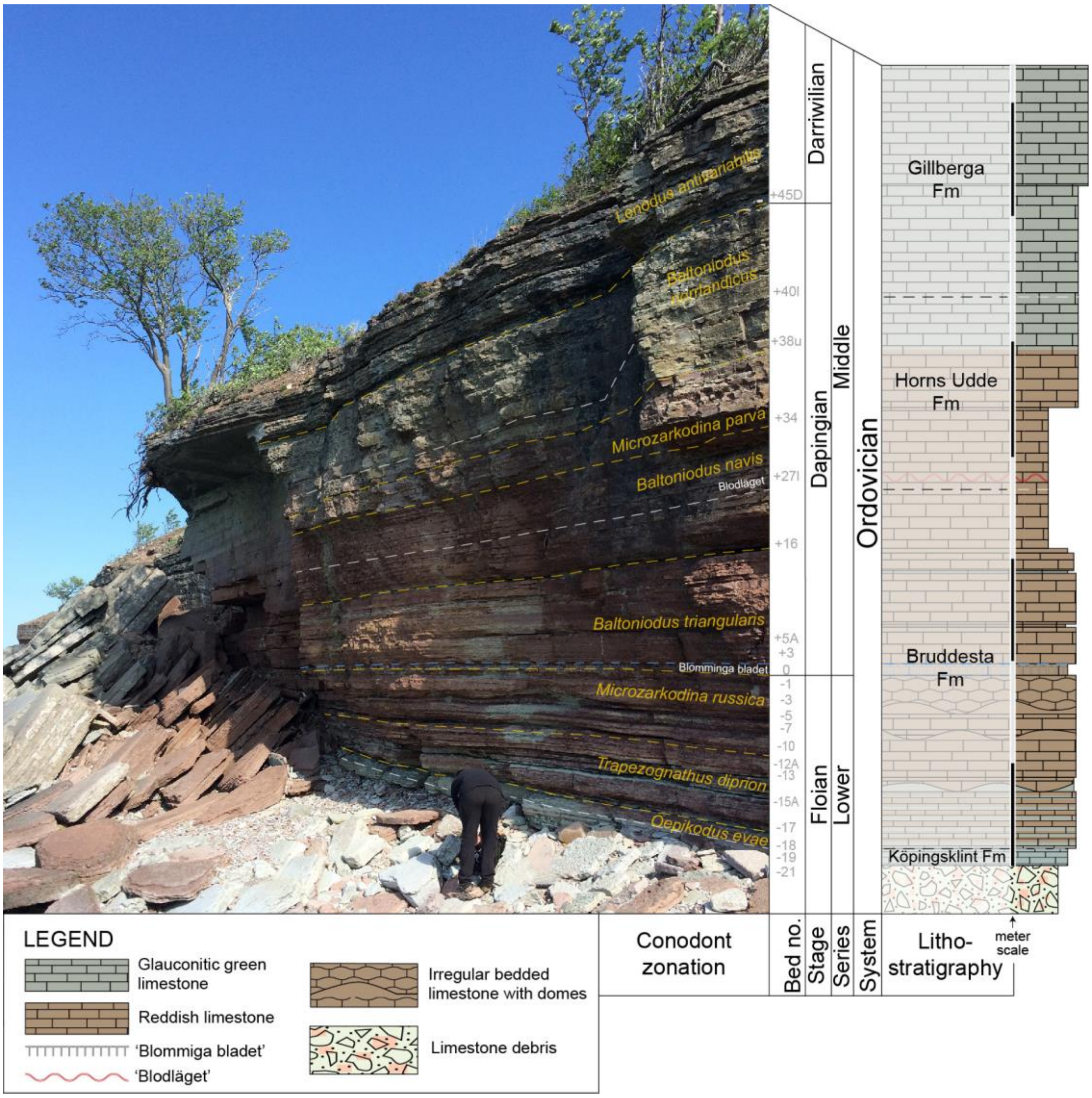

Figure 4: *Field photo of the locality at Horns Udde North, northern Öland. Lithological units and boundaries are shown in white. Conodont biostratigraphical zonal boundaries based on Bagnoli & Stouge (1997) are shown in orange and tied to global stratigraphy (left). The bed numbering system applied in the current study is also shown. The idealized log (right) shows main lithological features, unit names and thickness of profile. See legend for details.*

The Lower to Middle Ordovician succession at the Horns Udde North section (Figure 4) was sub-divided into eight conodont zones by Bagnoli & Stouge (1997) and van Wamel (1974) and partitioned into 101 beds, including sub-beds, from which brachiopods were collected. This has allowed for detailed bed-by-bed correlation tied accurately to the conodont biostratigraphy through the roughly nine-meter-thick section.

3.1.2 Horns Udde South section

This locality is located at the Cape of Horns Udde. The succession covers the top of the Horns Udde Formation and reaches approximately two meters higher into the overlying Gillberga Formation than the section North of Horns Udde. The succession starts with the reddish-colored Horns Udde Formation, of which the *B. navis*, *M. parva* and *B. norrlandicus* conodont zones are found (Figure 5). About midway through the latter conodont zone lies the formational boundary between the Horns Udde and the Gillberga formations.

Figure 5: *Field photo of the auxiliary section, Horns Udde South, northern Öland. Lithological units and boundaries shown in white and conodont biozones of Bagnoli & Stouge (1997) in orange. Bed numbering system is also indicated at unit boundaries.*

The Gillberga Formation is lithologically similar to the Horns Udde South section (see above), being greyish–green and unevenly bedded. It is about 4.1 m thick at this locality, thus potentially yielding up to two meters of new section compared to the section North of Horns Udde. Towards the top of this section, abundant glauconite grains characterize the rocks. Although the upper beds did not yield diagnostic conodont elements to aid biostratigraphic assignment, the associated brachiopod fauna is very characteristic of the lowermost Kunda Regional Stage. We are therefore confident that these beds are coeval with the *L. variabilis*

264

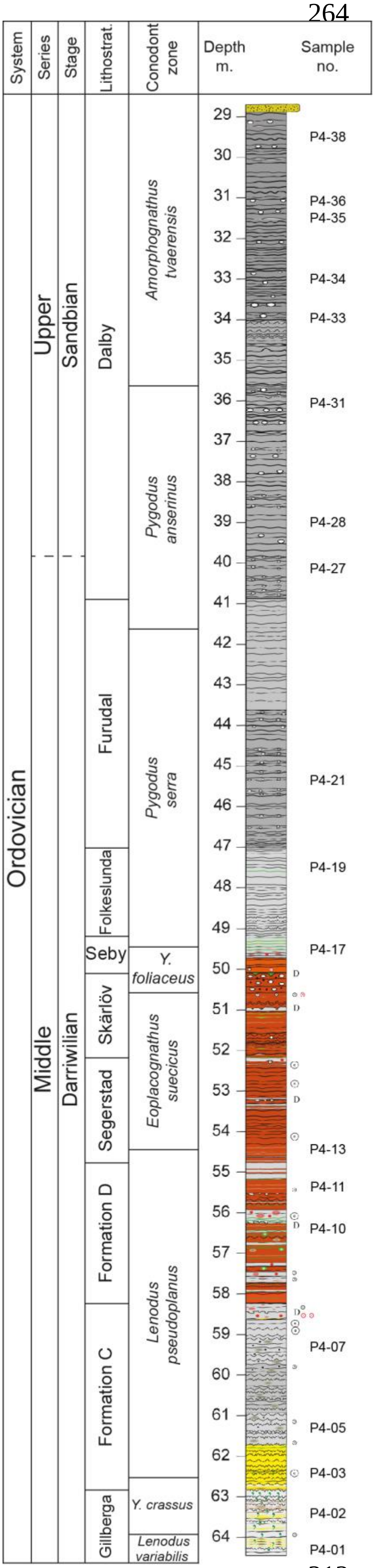

312

Conodont Zone. In this section, the Gillberga Formation was sampled from its base and divided into 32 beds, all of which yielded brachiopods.

3.1.3 Kårehamn P4 drill core

The sampled Kårehamn P4 core was drilled ca. 5 km offshore and to the east of the Kårehamn harbor (Figure 1). The borehole penetrated about 40 m of Ordovician limestone covering Middle and lower Upper Ordovician strata (middle Darriwilian to upper Sandbian) and the succession is typical for the Baltoscandian Paleobasin (Figure 6). The detailed description of the core is not published and work on the succession is still in progress. The base of the drillcore (at -64.5 m below the sea floor) is characterized by the upper part of the glauconite-bearing Gillberga Formation (Figure 6) and is thus, stratigraphically very close to the interval covered by the section at Horns Udde South. It is within the upper *L. variabilis* Conodont Zone and is immediately followed by the *Yangtzeplacognathus crassus* Conodont Zone (Dw2, Middle Ordovician). The strata from -62.9 m to -54.9 m (Formations C and D) are referred to the *Lenodus pseudoplanus* Conodont Zone (with the *Microzarkodina hagetiana* and *M. ozarkodella* subzones, Dw2). The overlying Segerstad and Skärlöv limestones (-54.8 to -50.2 m) are referred to the *Eoplacognathus suecicus* Conodont Zone *s.l.* The *Yangtzeplacognathus foliaceus* Conodont Zone (-51.1 to -49.6 m) is recorded from, and characterizes, the strata that are assigned to the Seby Limestone. There is a minor hiatus near the base of the *P. serra* Zone that is marked by a prominent discontinuity surface (D at -50.1 m on Figure 6). The *Eoplacognathus reclinatus* and *E. robustus* subzones of the *Pygodus serra* Conodont Zone are recorded from the Folkeslunda and Furudal limestones.

Figure 6: *Lithology and sample levels of the Kårehamn P4 core tied to bio-and lithostratigraphy. The lithostratigraphical names are mainly informal with some of the units either being topo-formations (e.g. Jaanusson, 1960), traditional units (e.g. Bohlin, 1949, 1953), or informal units (Stouge, 2004). Conodont biozonation established by GB and SS. Note the sampling levels for the current study on the far right.*

The lower 19.1 m of the core is assigned to the Orthoceratite limestone, which concludes with the Folkeslunda Limestone at -47 m (Figure 3; 6). The *Pygodus serra* Conodont Zone starting from the Folkeslunda Limestone represents the base of the uppermost third of the Darriwilian Stage (Dw3, upper Middle Ordovician). The *Pygodus anserinus* Conodont Zone is recorded from -41.7 m near the base of the Dalby Limestone and is succeeded by the *Baltoniodus variabilis* Subzone of the *Amorphognathus tvaerensis* Conodont Zone.

The top of the core (-29 m) is within the lower upper Sandbian (Upper Ordovician) Dalby Limestone (Figure 6). The *Amorphognathus tvaerensis* Zone and the *Baltoniodus variabilis* Subzone encompass this unit and extend to the top of the core. The base of the Upper Ordovician Series (Sandbian Stage) is tentatively placed ca. at – 39.8 m in the core (Figure 6). The core was sampled for brachiopods at one-meter resolution and nineteen beds yielded samples that could be analyzed (Figure 6).

3.1.4 Degerhamn Quarry

The Degerhamn Quarry (Figs. 1, 7) is an active limestone quarry, which is accessible by permission of the company that operates the quarry. The complete succession in the quarry extends down to the Cambrian Alum Shale Formation (Stouge, 2004), however, today this is covered by water. The exposed portion in the active quarry comprises the Gillberga Formation, which is composed of bedded, grey limestone superposed by various colors extending from green, red to violet. The overlying grey to green marker, locally known as ‘Sphaeronites’ bed, ca. 0.9 m thick, is composed of grainstone to packstone containing accumulations of ‘*Echinosphaeronites*’ in the middle of the unit (Stouge, 2004; see Figure 7). The coeval bed in south-central Sweden is referred to as the Täljsten (Eriksson et al., 2012). The upper part of the quarry consists of grey to mottled red or red-brown limestone.

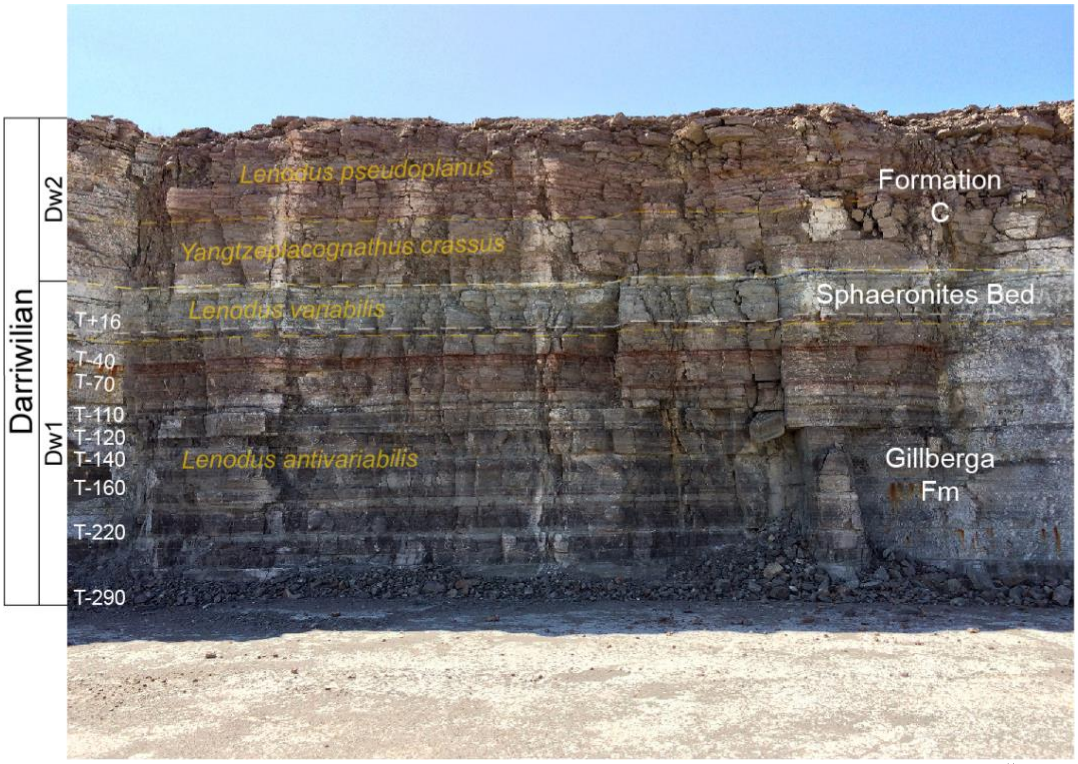

Figure 7: *Field photo showing the studied outcrop in the Degerhamn Quarry, South Öland. Lithological units and informal names written in white with corresponding white punctuated lines. Conodont biozonation, based on Stouge (2004) and Stouge & Bagnoli (2014), highlighted in orange with corresponding punctuated lines. The stratigraphical position of the samples obtained from this section is shown in white. The section is ca. 5 meters thick.*

The exposed succession in the active quarry is of Darriwilian age (Stouge, 2004; Stouge & Bagnoli, 2014). The lower part, composed of grey multi-colored limestone, is referred to the *Lenodus antivariabilis* and *L. variabilis* zones. The green-grey 'Sphaeronites' bed is referred to the *L. variabilis* zone up to the accumulation of '*Echinosphaeronites*', which is in the *Y. crassus* Conodont Zone. The upper part of the succession exposed in the quarry is assigned to the *Microzarkodina hagetiana* subzone of the *Lenodus pseudoplanus* Zone. From this locality, nine samples were collected through the *L. antivariabilis* to *L. variabilis* interval, and they are thus, all placed within the Middle Ordovician Darriwilian Stage (Dw1). Importantly, this locality provides samples from more deeply buried rocks ca. 100 km South of the other three studied localities. Thus, enabling the assessment of potential diagenetic impact by burial depth on carbon and oxygen isotope compositions within the *L. antivariabilis* Conodont Zone across Öland.

4 Materials and Methods

Fossil brachiopods (n = 185) and whole rock samples (n = 156) were collected from the localities described above (Figs. 1; 4–7). Samples from the Horns Udde North and South sections were collected bed-by-bed. The distance between the samples from the Degerhamn Quarry section, South Öland, varies, but is about 40 cm. Fossil brachiopods, as well as the bulk carbonate in which they were embedded, were collected at approximately one-meter intervals from the Kärehamn P4 core (Figure 1). All analyzed material are stored at the Natural History Museum of Denmark.

4.1 Sampling routines

Some brachiopods were sampled multiple times, hence, the total number of processed samples for geochemical and isotopic analysis is 226 brachiopod and 169 bulk rock samples. Brachiopods were cleaned using a brush and inspected for preservation under a binocular microscope. Splinters from the secondary shell layer of brachiopods were collected using a stainless-steel needle. Whole rock powder was extracted from the matrix adjacent to the sampled brachiopod shells using a handheld drill with a diamond-coated steel bit of ca. 1 mm diameter under a microscope. Rock surfaces were mechanically abraded, and powder was extracted from the rock matrix, avoiding weathered parts and calcite veins.

4.2 Scanning electron microscopy (SEM)

Shell splinters from the secondary shell layer of brachiopods were checked for textural preservation using SEM (Figure 8). Shell splinters were mounted on an adhesive stub and subsequently gold coated before screening. SEM analysis was conducted at the Natural History Museum of Denmark using a FEI Quanta 250 SEM in high vacuum mode.

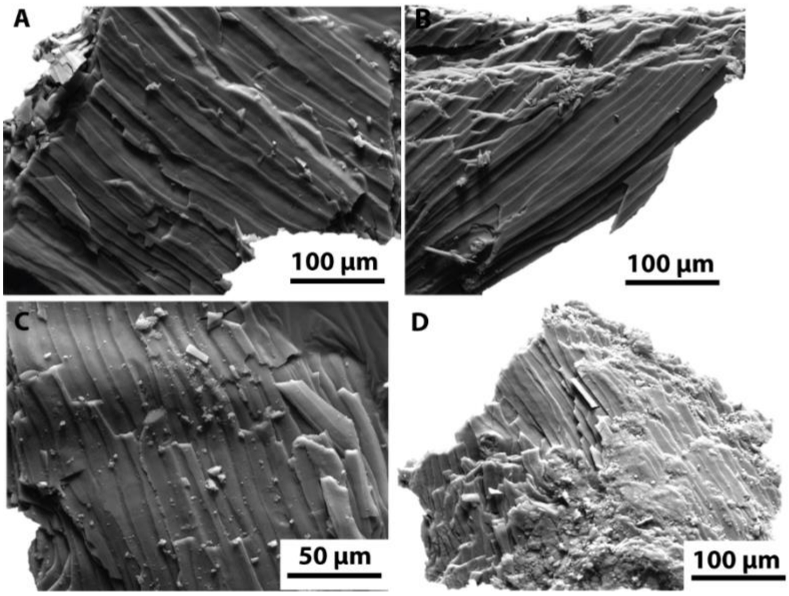

Figure 8: *SEM images of Ordovician brachiopod shell material.* ***a****) Sample OLH-19, mid Floian, Köpingsklint Formation, Horns Udde North.* ***b****) OLH-64, mid Dapingian, Horns Udde Formation, Horns Udde North.* ***c****) Sample OLK-3, upper Darriwilian, Folkeslunda limestone, Kärehamn P4 core.* ***d****) OLH-98, lower Darriwilian, Gillberga Formation, Horns Udde North. Specimens a, b and c show texturally well-preserved secondary shell layers and specimen d is characterized by partial recrystallization.*

4.3 Carbon and oxygen isotopes

Carbon and Oxygen isotope measurements of brachiopod shell material and whole rock powder were generated using an IsoPrime triple collector Gas Source Isotope Ratio Mass Spectrometer with a Multiflow unit at the University of Copenhagen following the procedures outlined by Ullmann et al. (2013). In summary, about 0.8 mg of sample material placed in glass vials were dissolved with ca. 0.05 ml of >100% concentrated phosphoric acid (H_3PO_4) and left to react for 90 minutes at 70°C. $\delta^{13}C$ and $\delta^{18}O$ compositions were measured from the resulting carbon dioxide. Data were corrected for weight-dependent biases by using the University of Copenhagen in-house reference standard – LEO (finely-crushed Carrara marble). Reproducibility of the measurements, as determined from the standard deviation of LEO is better than 0.1‰ for $\delta^{13}C$ and $\delta^{18}O$.

4.4 Element/Ca ratios

Element/Ca ratios (Sr/Ca and Mn/Ca) were measured from the reacted carbonate remains of brachiopod subsamples using an Agilent 5110 VDV Inductively Coupled Plasma Optical Emission Spectrometer (ICP-OES) at the University of Exeter, Penryn Campus following the procedure outlined in Ullmann et al. (2020). Accuracy of the analysis was controlled through multiple analyses of a synthetic quality control solution – BCQC (n = 4) and the international reference materials – AK (n = 8) and JLs-1 (n = 12). Analytical bias, determined via the deviation of measured element/Ca ratio from the expected value in the gravimetrically prepared quality control solution – BCQC, was ≤ 0.5% for each of the reported element/Ca ratios.

5 Results

All carbon and oxygen isotope compositions of brachiopods and bulk rocks and their relations to their element/Ca ratios are summarized in Figure 9 and all data are presented in Supplementary information Figure 2, as well as the Supplementary datafile. In Figure 9, the new data are plotted together with literature data from well-preserved coeval samples from the eastern part of the Baltoscandian Paleobasin (St. Petersburg region, Rasmussen et al., 2016).

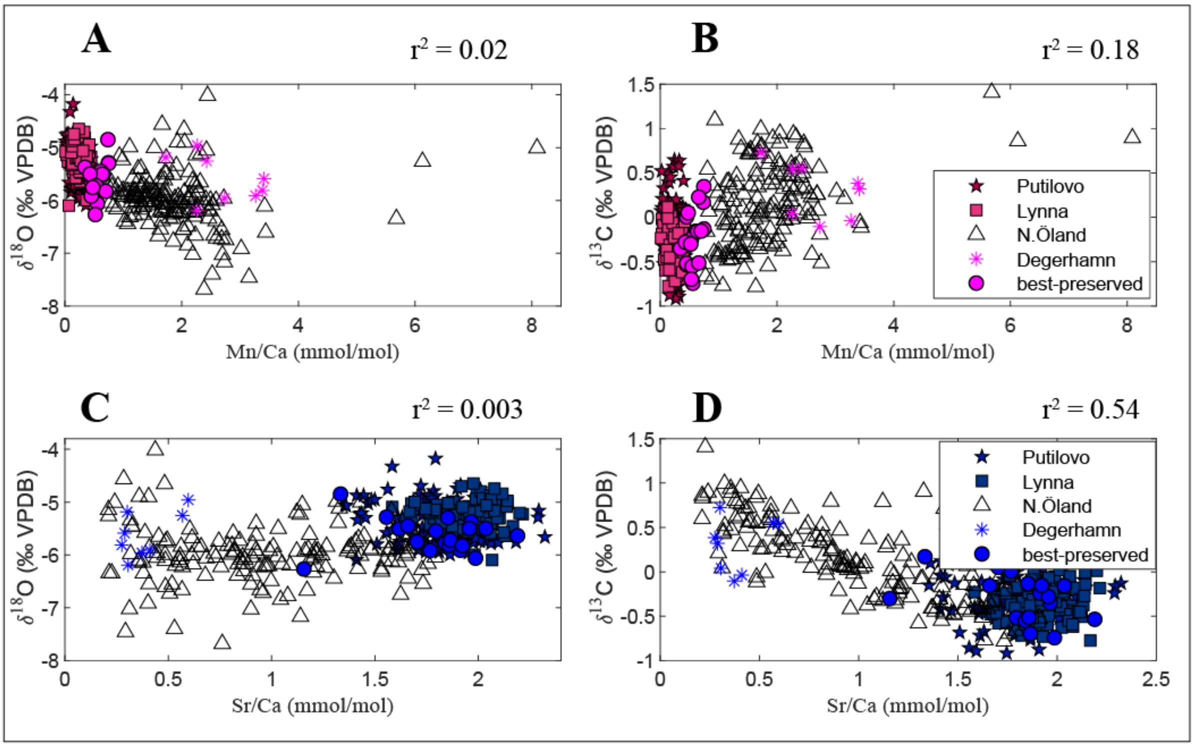

Figure 9: *Scatter plots showing correlation between element/Ca ratios and $\delta^{18}O$ and $\delta^{13}C$ values of investigated brachiopods in the current study and the east Baltic dataset (Putilovo and Lynna, C. M. Ø. Rasmussen et al., 2016). Element/Ca data interpreted as best-preserved if Mn/Ca ≤ 1. N. Öland = North Öland. Values of r^2 only refer to the Öland dataset.*

5.1 Carbon isotopes

Carbon isotope values of brachiopods ($\delta^{13}C_{brachiopod}$) vary between -0.78‰ and +1.41‰ and whole rock carbonates ($\delta^{13}C_{bulk}$) between -1.01‰ and +1.57‰. Both datasets follow the same general temporal trend (Figure 10). $\delta^{13}C_{brachiopod}$ values are generally lighter than $\delta^{13}C_{bulk}$, being offset by approximately 0.5‰. Both $\delta^{13}C_{brachiopod}$ and $\delta^{13}C_{bulk}$ are characterized by an increasing trend during the Floian, showing a range of -0.3‰ to +1.0‰. This is followed by a decline of about 1.7‰ in $\delta^{13}C_{brachiopod}$ from the Floian–Dapingian transition to the end of the Dapingian (*B. triangularis* to the top of the *B. norrlandicus* conodont zones). For $\delta^{13}C_{bulk}$, the decrease is less severe as $\delta^{13}C$ values only plunge by ca. 0.8‰ before stabilizing in the lower Darriwilian *L. antivariabilis* Conodont Zone to +0.3‰. Beginning in the *Y. crassus* Conodont Zone, a positive excursion takes place in both $\delta^{13}C_{brachiopod}$ and $\delta^{13}C_{bulk}$ which culminates in the middle Darriwilian *E. suecicus* Conodont Zone. Here, peak values of +1.4‰ and +1.6‰ are recorded for $\delta^{13}C_{brachiopod}$ and $\delta^{13}C_{bulk}$ respectively. Subsequently, in the upper Darriwilian and Sandbian, $\delta^{13}C_{brachiopod}$ and $\delta^{13}C_{bulk}$ values decrease by ca. 0.6‰ but remain heavier than during pre-excursion times, ranging between +0.2‰ and +1.0‰.

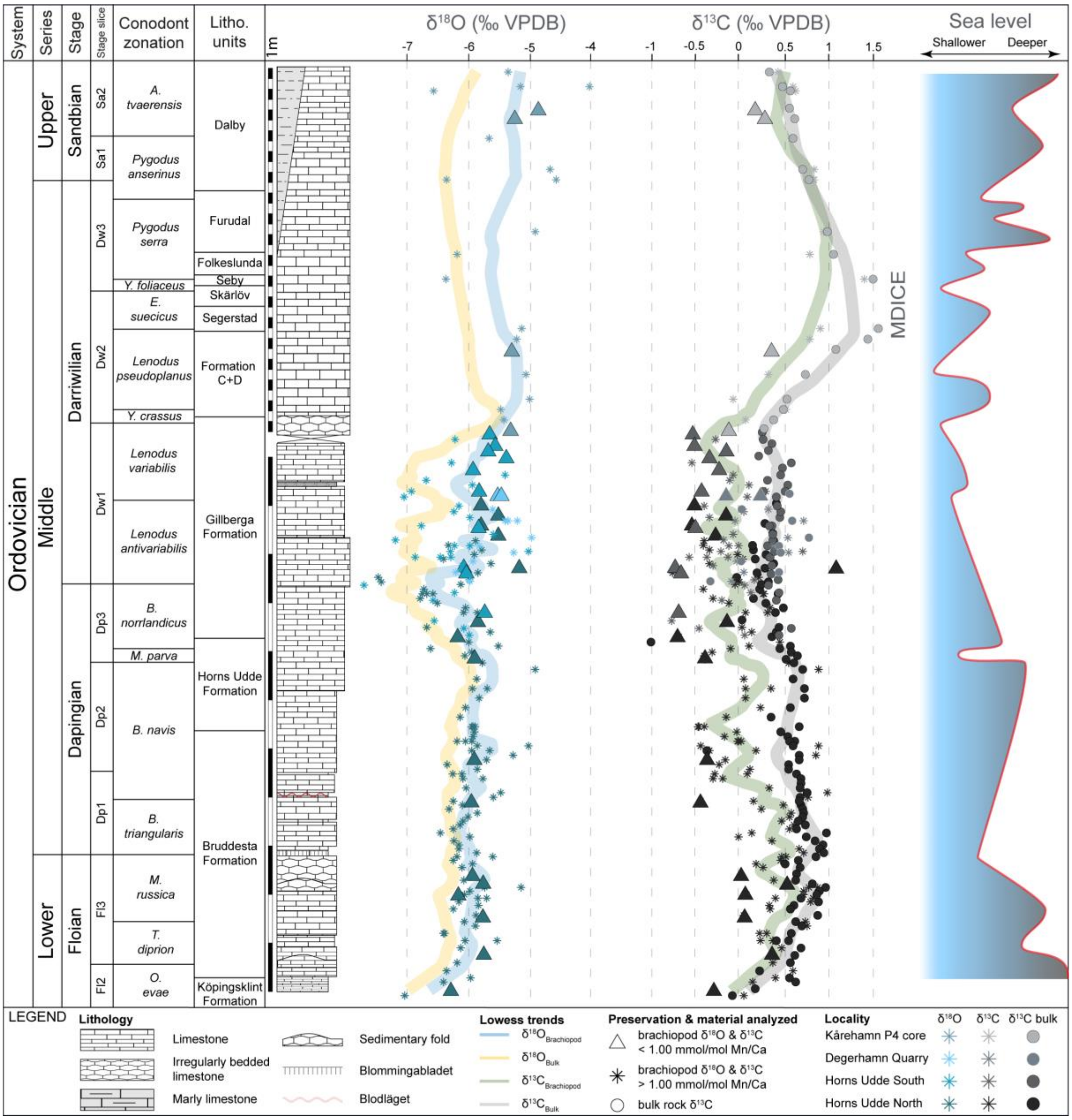

Figure 10: *Summary figure showing carbon and oxygen isotope compositions of investigated fossil brachiopods and bulk carbonates through the studied composite interval as well as our interpreted relative sea level curve up through the succession (based on lithology and conodont biofacies (see Bagnoli & Stouge (1996)). The four different localities studied are represented by their own shading. A 10-point Lowess smoothing has been applied to accentuate temporal trends in the dataset using the software OriginPro. Yellow Lowess curve represents bulk oxygen values shown in Supp. Fig 2. A pronounced positive $\delta^{13}C$ excursion is apparent in both bulk carbonates and fossil brachiopods during the Middle Darriwilian (MDICE), as well as a sustained Darriwilian increase in $\delta^{18}O$. Note that samples below the operational limit of preservation all fall within the range of the samples above the cutoff limit and that the dataset is not evenly scaled. The mid-Darriwilian to Sandbian part of the figure is vertically compressed due to reduced sampling resolution in this interval.*

5.2 Oxygen isotopes

The oxygen isotope record exhibits a general long-term Ordovician increasing trend and most notably, a sustained rise during the Darriwilian (Figure 10). Brachiopod $\delta^{18}O$ values are typically offset by +0.6‰ relative to $\delta^{18}O_{bulk}$ (see supp. Figure 2) and vary by up to 1‰ within individual brachiopod beds. Bulk rock $\delta^{18}O$ composition ranges from -8.0‰ to -4.9‰ in the studied interval and between -7.7‰ and -4.0‰ for brachiopods. The Floian is characterized by an increase of up to 1.8‰ in both brachiopods and bulk rocks, before reverting to background values of about -6‰ at the Floian–Dapingian transition (*B. triangularis* Conodont Zone). The Dapingian dataset is characterized by an initial increase of ca. 1.5‰ in both $\delta^{18}O_{bulk}$ and $\delta^{18}O_{brachiopod}$, followed by a decrease of up to 2‰ reaching into the lower Darriwilian. Within the lower Darriwilian (*L. antivariabilis* Conodont Zone), both brachiopods and bulk rocks display a wide $\delta^{18}O$ range of 1.9‰ and 3.0‰ respectively. Notably, the lowest $\delta^{18}O$ values in this interval correspond to samples from North Öland, whereas those from Degerhamn, South Öland, are characterized by the heaviest $\delta^{18}O$ values. Beginning in the *L. variabilis* Conodont Zone, brachiopod $\delta^{18}O$ values steadily increase by up to 1.5‰ into the lower *E. suecicus* Conodont Zone. This is followed by a decrease of ca. 1‰ until the base of the *P. serra* Conodont zone (upper Darriwilian). Subsequently in the upper Darriwilian to Sandbian (*P. serra* to *A. tvaerensis* Conodont Zone) interval, $\delta^{18}O$ values of bulk carbonates and brachiopods show no clear pattern, but instead vary significantly by up to 2.5‰.

5.3 Element/Ca ratios

Element/Ca ratios of investigated brachiopods vary between 0.21 and 2.19 mmol/mol for Sr/Ca and 0.34–8.09 mmol/mol for Mn/Ca. Element/Ca ratios do not vary distinctly between localities and generally, and do not display discernible stratigraphic trends (Supplementary information Figure 1). Correlation between element/Ca ratios and isotopic compositions is observed in the case of Sr/Ca and $\delta^{13}C$ (Supplementary information Figure 3), with negative slope of $\Delta^{13}C$ (the difference of brachiopod and bulk carbonate $\delta^{13}C$) vs Sr/Ca and $\delta^{13}C$ vs Sr/Ca suggesting a link between depletion in Sr/Ca and $\delta^{13}C$. These element/Ca trends diverge from those documented for the Eastern Baltic (Figure 5; (C. M. Ø. Rasmussen et al., 2016), hinting at variability in trace element patterns in sediments within the Baltoscandian Paleobasin.

6 Discussion

6.1 Screening of samples

A combination of optical (Scanning Electron Microscopy), chemical (element/Ca ratios) and statistical methods (correlation between element/Ca ratios and $\delta^{13}C$, $\delta^{18}O$) have been applied to assess the fidelity of the carbon and oxygen isotope data presented herein (see supplementary information).

Generally, brachiopods with Mn/Ca ratio of ≤ 1 mmol/mol show well-preserved shell ultrastructure and usually exhibit Sr/Ca ratios ≥ 1.3 mmol/mol, which is comparable to values reported for well-preserved early Paleozoic biogenic calcite (C. M. Ø. Rasmussen et al., 2016; Steuber & Veizer, 2002). Therefore, these brachiopods probably represent the best-preserved samples in our dataset. Importantly, the secular Ordovician carbon and oxygen isotope trend herein recorded from Öland remains unchanged whether or not only samples below a particular element/Ca ratio preservation limit (e.g. ≤ 1 mmol/mol Mn/Ca) are considered (Figure 10), which is similar to the conclusion reached by Veizer et al. (1999) and more recently by Goldberg, Present, Finnegan, & Bergmann (2021).

6.2 Carbon Isotopes

Over the last three decades, the carbon isotope stratigraphy of Baltoscandian Ordovician successions has been extensively documented, albeit mainly based on bulk rock carbonates (e.g. Ainsaar et al., 1999, 2004, 2007, 2010; Bauert et al., 2014; Calner et al., 2014; Kaljo et al., 2007; Lindskog et al., 2019; Wu et al., 2017) (Figure 11). This has enabled the identification of early Paleozoic carbon isotope excursions which have been used as important stratigraphic correlation tools, for instance the MDICE (Ainsaar et al., 2010; Ainsaar, Meidla, & Tinn, 2004; Ainsaar, Tinn, Dronov, Kiipli, & Radzevicius, 2020; Kaljo, Martma, & Saadre, 2007; M. R. Saltzman & Edwards, 2017; Schmitz, Bergström, & Xiaofeng, 2010; Young, Gill, Edwards, Saltzman, & Leslie, 2016). In one of the first studies to devote attention to the Early Ordovician interval in Baltoscandia, Calner et al. (2014) investigated the upper Tremadocian to middle Darriwilian $\delta^{13}C$ record of the Orthoceratite limestone of Öland, Sweden and made comparisons to that of the Argentine Precordillera. They reported a negative excursion (ca. 1‰) in the basal parts of the Köpingsklint Formation and a marked positive excursion in the *O. evae* Conodont Zone and proposed that these Early Ordovician excursions constitute valuable chemostratigraphic markers.

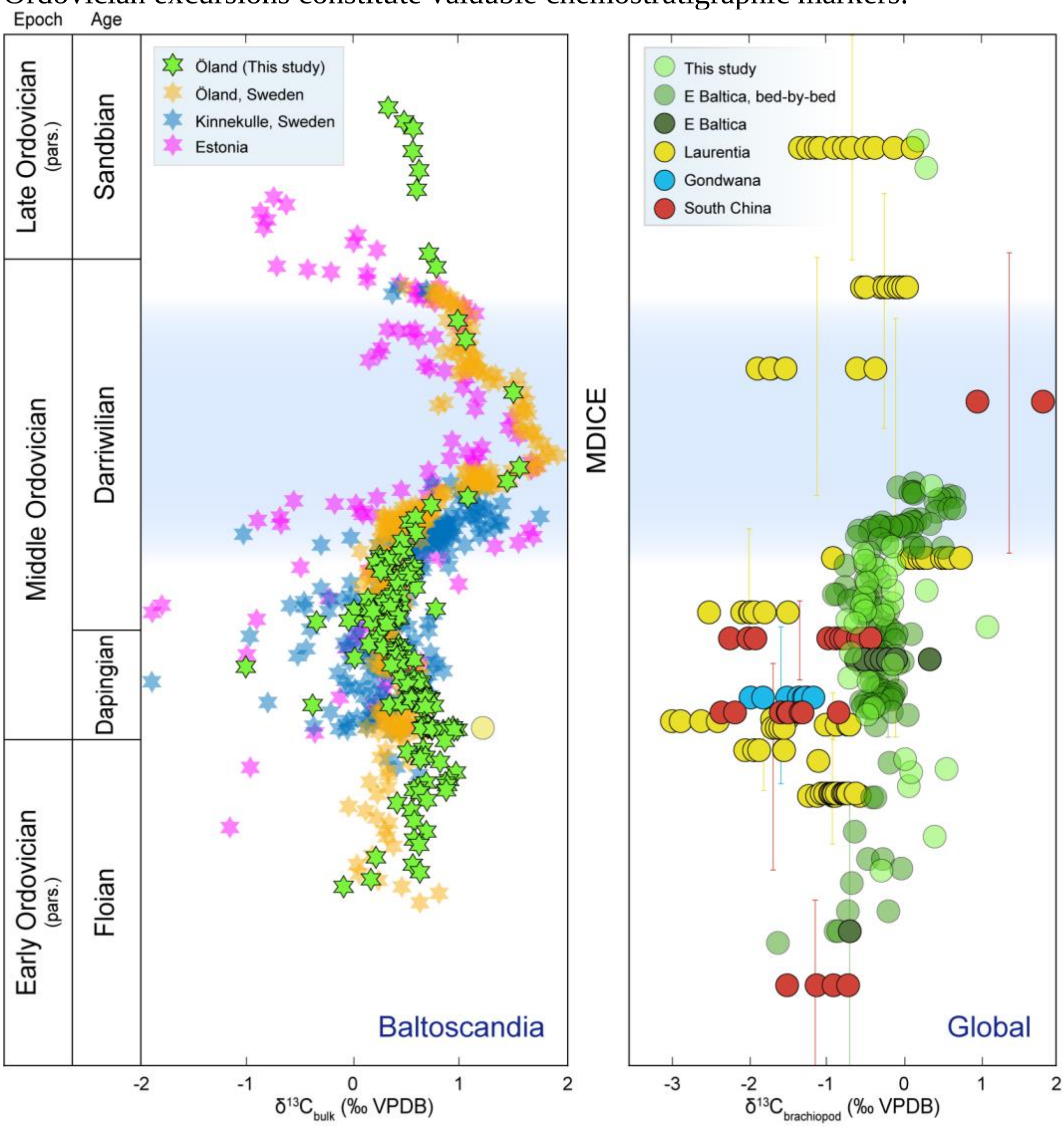

Figure 11: *Comparison of regional and global whole rock carbonate and brachiopod $\delta^{13}C$ trends. Whole rock $\delta^{13}C$ data ($\delta^{13}C_{bulk}$) all originate from Baltoscandia (left figure): Öland (Wu et al., 2017); Kinnekulle (Lindskog et al., 2019); Estonia (Kaljo et al., 2007).*

Brachiopod $\delta^{13}C$ data (right figure) elucidate Baltoscandia $\delta^{13}C$ trends using best-preserved brachiopods (Mn/Ca ≤ 1 mmol/mol) from this study in conjunction with data from C. M. Ø. Rasmussen et al. (2016) compared to reported $\delta^{13}C$ trends from global compilations (Qing & Veizer, 1994; Shields et al., 2003; Veizer et al., 1999; Veizer & Prokoph, 2015). Note the marked MDICE trend in both curves, as well as the temporal resolution of the Baltic brachiopod bed-by-bed dataset as compared to the global sites. Vertical bars in the right diagram denote stratigraphical uncertainty of the global compilation samples highlighted in corresponding colors. This temporal constraint is based on either the provided lithostratigraphical information in the source references using C. M. Ø. Rasmussen et al. (2019) or biostratigraphy, based on brachiopod species ranges where possible (St. Petersburg: Egerquist (2004), Yangtze Platform: Zhan, Jin, & Chen (2007)).

Lehnert, Meinhold, Wu, Calner, and Joachimski (2014) documented the presence of three notable short-term negative $\delta^{13}C$ excursions in the Lower to Middle Ordovician and proposed new names for $\delta^{13}C$ excursions encompassing the Cambrian–Ordovician boundary to the lowermost Darriwilian interval. C. M. Ø. Rasmussen et al. (2016) reported $\delta^{18}O$ and $\delta^{13}C$ records of the Floian to mid-Darriwilian interval in eastern Baltoscandia based on bed-by-bed brachiopod samples from Russia. Subsequently, Wu et al. (2017) documented a complete record of the MDICE (rising limb, peak interval and falling limb) and reported that it spans the *L. pseudoplanus*, *E. suecicus*, *P. serra* and *P. anserinus* conodont zones. Thus, the Lower to Middle Ordovician carbon isotope stratigraphy of Baltoscandia is well-constrained based on bulk rock data.

In the present study, the significant carbon isotope excursion, discernible in both brachiopods and bulk carbonate, is the MDICE with a magnitude of ca. 1‰ and peak values around +1.5‰ (Figure 11). The peak of this isotope event is at -54.8 to -52.4 m of the Kårehamn core, corresponding to the *E. suecicus* Conodont Zone (Figure 10). There is overall agreement between bulk rock and brachiopod $\delta^{13}C$ trends (Figs. 10; 11), with about 0.5‰ lighter $\delta^{13}C_{brachiopod}$ values. The similarity of both trends is consistent with observations that over specific time intervals, brachiopod and bulk rock $\delta^{13}C$ records show good correlation, but some deviations exist (Brand, 2004; Munnecke, Calner, Harper, & Servais, 2010). Primary inter- and intra-specific variability of $\delta^{13}C$ is documented in literature for ancient (e.g. Korte and Hesselbo, 2011; Korte et al., 2005; Veizer et al., 1999) and modern brachiopods (e.g. Takayanagi et al., 2013, 2015; Ullmann et al., 2017) and are linked to pronounced seasonality of the shallow marine depositional environment, metabolism-mediated or kinetic fractionation effects (Auclair et al., 2003; Korte et al., 2005, 2017; Takayanagi et al., 2015). The smooth trend evident in the current $\delta^{13}C_{bulk}$ record, however, can be explained by the mixing of microscopic-sized carbonate fragments in the micritic carbonates, which yield homogenized $\delta^{13}C$ compositions and consequently, generated the smoothed isotope curves that can display $\delta^{13}C$ high-frequency variability (cf. Korte et al., 2017). In addition, variations in $\delta^{13}C$ values of dissolved inorganic carbon (DIC) in the open ocean are relatively small (Swart, 2015) and the present Baltoscandia $\delta^{13}C$ record therefore probably reflects the $\delta^{13}C$ composition of Ordovician open ocean DIC.

6.2.1 Regional and global comparison of the Baltoscandian $\delta^{13}C$ record

The 0.5‰ offset between $\delta^{13}C_{brachiopod}$ and $\delta^{13}C_{bulk}$ in the current study seems to be a consistent pattern throughout the Baltoscandian Paleobasin. Specifically, Floian to Sandbian $\delta^{13}C_{bulk}$ values from different parts of Baltoscandia (Figure 11) show a range between -1‰ and +2‰ (Kaljo et al., 2007; Lindskog et al., 2019; Wu et al., 2017). For fossil brachiopods, values ranging between -1‰ and +1‰ have been reported for the eastern Baltoscandian Paleobasin (e.g. Bergmann et al., 2018; C. M. Ø. Rasmussen et al., 2016) and these are comparable with our observations (Figure 6). Floian–Sandbian $\delta^{13}C_{bulk}$ range between -1.0‰ and +1.6‰, and best preserved $\delta^{13}C_{brachiopod}$ values (with Mn/Ca ≤ 1 mmol/mol) range between -0.7‰ and +0.4‰. This offset may reflect a basin configuration where deeper waters are ^{13}C-depleted and the upper parts are ^{13}C-enriched due to transport of organic matter to deeper waters (Kroopnick, Margolis, & Wong, 1977; van de Schootbrugge, Föllmi, Bulot, & Burns, 2000). However, this is unlikely to be the case as the Baltoscandian Paleobasin was characterized by very low relief (Jaanusson, 1973) and thus, no significant differences in water depth in the sea. The lighter $\delta^{13}C$ values in brachiopods compared to the bulk rock data potentially reflects species-specific carbon isotope fractionation (vital effects). Comparison of the new Baltic $\delta^{13}C_{brachiopod}$ record to published data and compilations (Shields et al., 2003; Veizer et al., 1999; Figure 11) reveals that the Baltoscandian record is characterized by generally heavier $\delta^{13}C_{brachiopod}$ values. This disparity can be attributed to local/regional differences in C isotope compositions, and this is in concert with data from several other sedimentary basins (Shields et al., 2003; Veizer et al., 1999) which have depositional environments and tectonic regimes different from those of the Baltoscandian Paleobasin (see supplementary information). Nevertheless, the apparent similarity in the trends of both $\delta^{13}C_{brachiopod}$ records strengthens the view that the Baltoscandian $\delta^{13}C_{brachiopod}$ reflect a near-primary record and a global trend.

6.3 Oxygen isotopes

The composite Baltic $\delta^{18}O$ record (Figure 12) reveals a secular Floian to Sandbian $\delta^{18}O$ increase of ca. 1.4‰. This is most apparent during the Darriwilian, where an increase of ca. 0.8‰ is recorded (Figure 10), mirroring the Early to Middle Ordovician $\delta^{18}O_{brachiopod}$ record from eastern Baltoscandia (C. M. Ø. Rasmussen et al., 2016; Figure 12). The similarity between these oxygen isotope records (Figure 12) thus suggests that the Baltoscandian Early to Middle Ordovician oxygen isotope record is spatially consistent and a primary geochemical signature. Although the late Darriwilian to Sandbian portion of this record is less constrained, data from the best-preserved brachiopods suggests that $\delta^{18}O$ values in that period remained at least as heavy as during middle Darriwilian times. This is congruent with published records indicating a transient cooling event at this time (Saltzman and Young, 2005; Vandenbroucke et al., 2010).

Furthermore, the Early to Late Ordovician Baltoscandian $\delta^{18}O$ record of the present dataset is consistent with the trend of increasing $\delta^{18}O$ values with decreasing age, and this has long been documented for the Ordovician (Grossmann and Joachmiski, 2020; Qing and Veizer, 1994; Shields et al., 2003, Veizer et al., 1999; Veizer and Prokoph, 2015). However, the current Baltic dataset provides improved temporal resolution compared to the global compilations, which have limited resolution in the Ordovician (see Figure 12 for comparison of datasets).

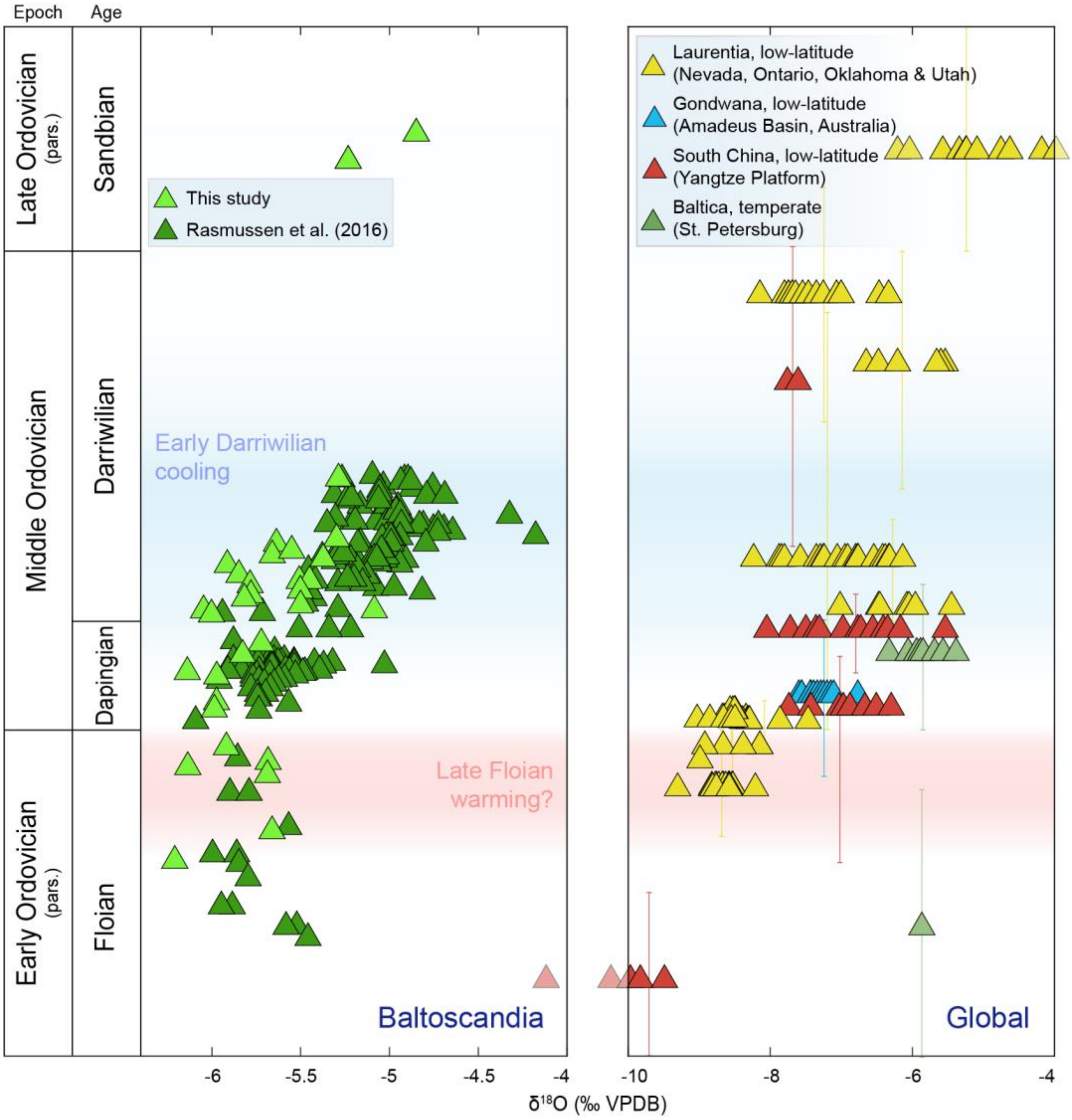

Figure 12: *Long-term comparison between Early Ordovician (Floian) to early Late Ordovician (Sandbian) brachiopod $\delta^{18}O$ values in Baltoscandia (based on pristine brachiopods) and global brachiopod $\delta^{18}O$ compilations. Both the Baltoscandian and global compilation datasets elucidate a general pattern of increasing brachiopod $\delta^{18}O$ values upwards, which is most prominent during the Middle Ordovician (compare with Figure 2 showing a similar trend based on the conodont apatite-derived curve of Trotter et al. (2008). Vertical bars in the right diagram denote stratigraphical uncertainty of the global compilation samples highlighted in corresponding colors. Note the well-resolved temporal resolution of the Baltic brachiopod bed-by-bed dataset as compared to the global data points. Global compilation dataset obtained from Qing & Veizer (1994), Veizer et al. (1999), Shields et al. (2003), Veizer & Prokoph (2015). Samples are temporally constrained as in Figure 11.*

6.3.2 Regional and global comparison of the Baltoscandian $\delta^{18}O$ record

The comparison of the Baltoscandian $\delta^{18}O$ record with global compilation data (Figure 12) indicates that the Baltoscandian record is characterized by heavier $\delta^{18}O$ values. This may be attributable to the paleogeographical position of Baltica during the studied interval, as well as the relatively shallow sedimentary burial – thus, reduced susceptibility to burial diagenesis – which largely characterized the Baltoscandian Paleobasin. The mid latitudinal positions, which Baltica occupied during the Early to Middle Ordovician (Torsvik et al., 2012) suggests that Baltoscandian brachiopods lived in cooler waters compared to their counterparts in more equatorial paleocontinents, which constitute the majority of the Ordovician global compilation data (Shields et al., 2003; Veizer et al., 1999) (Figure 12). For instance, the paleocontinent of Laurentia was located in equatorial realms throughout the Ordovician while Baltica only approached equatorial paleolatitudes during the Late Ordovician (Kaljo et al., 2007).

6.4 Paleoenvironmental significance of the Baltoscandian oxygen isotope record

Temporal variation in $\delta^{18}O$ of biogenic calcite can be influenced by several factors including changes in seawater $\delta^{18}O$ composition, temperature of calcite precipitation, vital effects, pH changes and diagenetic alteration of near-primary brachiopod $\delta^{18}O$ (Bruckschen & Veizer, 1997; Munnecke et al., 2010; Qing & Veizer, 1994; Swart, 2015). Climatic cooling has been invoked as an explanation for the Ordovician $\delta^{18}O$ trend observed in both brachiopods and conodonts, and cooling, in turn, has been associated with the coinciding GOBE (Qing and Veizer, 1994; C. M. Ø. Rasmussen et al., 2016; Trotter et al., 2008). Alternative interpretations have also been postulated for this trend including changes in the oxygen isotope composition of seawater (Jaffrés et al., 2007; Shields et al., 2003) and diagenetic alteration (Bergmann et al. 2018).

In the current Baltoscandia record, vital effects are unlikely to explain the secular $\delta^{18}O$ trend because the secondary layer of brachiopod shells, which are more likely to have been secreted in isotopic equilibrium with or very close to the seawater were utilized (Carpenter & Lohmann, 1995; C. Ullmann, Frei, Korte, & Lüter, 2017). Although the $\delta^{18}O$ values during the early Darriwilian and late Darriwilian to late Sandbian portion of the Öland data show a wide range (Figure10) suggesting that diagenesis has modified some of the primary $\delta^{18}O$ compositions, the best-preserved samples (Figure 10, 12), however, show a long-term trend which is consistent with the $\delta^{18}O$ LOWESS smoothing line and narrow $\delta^{18}O$ range (Figure 10), indicating that the near-primary $\delta^{18}O$ trends are preserved (see also section 6.1).

Besides the influence of significant ice-volume changes, seawater $\delta^{18}O$ composition may become heavier through high-temperature reactions of seawater with silicate minerals in hydrothermal systems associated with oceanic ridges and their flanks (Veizer and Prokoph, 2015; Verard and Veizer, 2019 and references therein). Results based on modelling efforts show that the maximum rate of change of the $\delta^{18}O$ composition of seawater due to high-temperature reactions is ca. 1‰ per 100 million years (Jaffrés et al., 2007; Veizer and Prokoph, 2015). However, the time-period covered by the current Baltic dataset is ca. 19 million years (Gradstein & Ogg, 2020), thus making it unlikely that seawater-silicate rock interactions could have been rapid enough to generate the observed $\delta^{18}O$ change.

Furthermore, clumped isotope results based on Middle Ordovician brachiopods have been reported to yield seawater $\delta^{18}O$ compositions between -0.9‰ and -1.2‰ (Bergmann et al., 2018), and this is comparable to $\delta^{18}O$ compositions of modern seawater.

Consequently, we interpret the long-term Baltoscandia $\delta^{18}O_{brachiopod}$ trend as dominantly reflecting a near-primary paleotemperature signal, in agreement with previous studies (Goldberg, Present, Finnegan, & Bergmann, 2021; C. M. Ø. Rasmussen et al., 2016; Trotter et al., 2008). In this scenario, the $\delta^{18}O$ trend represents a transition from warmer climatic conditions during the Early Ordovician to less-warm conditions during the Early to Middle Ordovician transition and a cooling episode during the Darriwilian which may have persisted into the Sandbian.

6.4.1 Middle Ordovician cooling

The composite Baltoscandia record (Figure 12) indicates a ca. 1.5‰ $\delta^{18}O_{brachiopod}$ increase between the Floian and mid-Darriwilian. Assuming a ~ 4 ºC temperature change for 1‰ $\delta^{18}O$ shift (Epstein and Mayeda, 1953), this is suggestive of a 6–7 ºC relative cooling within a period of ca. 8 million years in an ice-free world even during the period with cooler temperatures is assumed (Gradstein & Ogg, 2020). This relative cooling is comparable to bio-apatite- and brachiopod-based estimates of sea surface temperature evolution during the same interval (Goldberg, Present, Finnegan, & Bergmann, 2021; Grossman and Joachimski, 2020; Trotter et al., 2008). The northward drift of Baltica towards the equator during the Ordovician (Torsvik et al., 2012) can be expected to have resulted in progressively lighter $\delta^{18}O$ values due to warming. However, the opposite trend is apparent in the $\delta^{18}O$ record. Therefore, the 1.5‰ amplitude of change in $\delta^{18}O_{brachiopod}$ potentially represents an under-estimation of the actual global seawater temperature change. Moreover, short-term sea level fall occurs in the upper part of the Dapingian, and a pronounced and long-lasting sea-level fall is observed both at the regional and global scale starting within the earliest Darriwilian, suggesting a good correspondence with the pronounced shift to heavier $\delta^{18}O$ values during the Mid-Ordovician (Figure 13). These observations support glacio-eustasy driven by climatic cooling and this would suggest that a portion of the $\delta^{18}O_{brachiopod}$ increase is related to ice volume effect and the temperature decline on Baltica was less that 6–7°C.

Biofacies analyses of brachiopods, conodonts and trilobites have all demonstrated that shallow-water faunas became ubiquitous in Baltoscandia during the early Darriwilian, indicative of falling sea level in the order of 150 m from the late Floian to the early Darriwilian (A. T. Nielsen, 1995; C. M. Ø. Rasmussen et al., 2016; J. A. Rasmussen & Stouge, 2018; Stouge et al., 2020). Also, prior to the Middle Ordovician, lighter $\delta^{18}O_{brachiopod}$ values during the late Floian (Figure 12) coincide with the late Floian migration of Laurentian warm-water conodont taxa into Baltoscandia (i.e. an influx of species typical of low-latitude regions), interpreted to denote a relatively brief warming episode. Hereafter follows the Middle Ordovician influx of temperate-water taxa denoting cooler waters (Bagnoli & Stouge, 1997; Stouge et al., 2020).

In addition to paleontological evidence, several sedimentological and cyclostratigraphical studies have argued for a global Darriwilian cooling (Cherns et al., 2013; Dabard et al., 2015; Fang et al., 2019; Lindström, 1984; Lindskog et al., 2014, 2019; Turner et al., 2012). Therefore, the discussion of whether the Middle Ordovician oxygen isotope trend is climate-related, or reflecting either diagenetic overprint (Bergmann et al., 2018) or changing seawater composition (Veizer & Prokoph, 2015) seems to overlook the point that climate is invoked as a main driver for this secular trend based on a whole suite of *other* proxies that independently from the oxygen isotope record indicate sea level fluctuations, and, in many cases, on a bed-by-bed scale (Figure 13). Of equal importance is the rapidity of these sea level oscillations such as those observed in the late Dapingian and in the *L. variabilis–Y. crassus* interval of the Darriwilian. As they occur in a stable intra-cratonic setting on Baltica, it is difficult to invoke other causal mechanisms than glacio-eustasy. We note, however, that high-frequency fluctuations in 4th order sea-level changes are only expressed in the late Dapingian and then again in the *L. variabilis* Zone to the *M. ozarkodella* Conodont subzones of the Darriwilian (Figure 13). Perhaps, this change in the expression of sea-level change is linked to distinct phases of ice-sheet growth, with high-frequency fluctuations particularly well-expressed in a late Dapingian phase that saw the onset of growth of continental ice with small volume ice-changes paced by orbital changes. The *L. antivariabilis* Zone, instead, may have been characterized by the establishment of a larger but stable ice sheet, less sensitive to high-frequency fluctuations. The return to more prominent high-frequency fluctuations in 4th order sea level changes in the *L. variabilis* Zone, and within the rest of the studied succession, could be due to a third phase of ice-sheet growth with a new increase in volume of continental ice occupying new areas that were particularly sensitive to ice growth and decay via orbital changes. Although this interpretation is highly speculative, it presents the merit to reconcile observed trends in sea-level change and $\delta^{18}O_{brachiopod}$ data.

A similar interpretation was suggested based on a sequence stratigraphical analysis of early Darriwilian sections from southern Jordan (Turner et al., 2012), as did model simulations which suggest that the climatic threshold for glacial onset was reached during the Darriwilian (Pohl et al., 2016 and references therein), in agreement with reported contemporaneous 3rd order eustatic cycles.

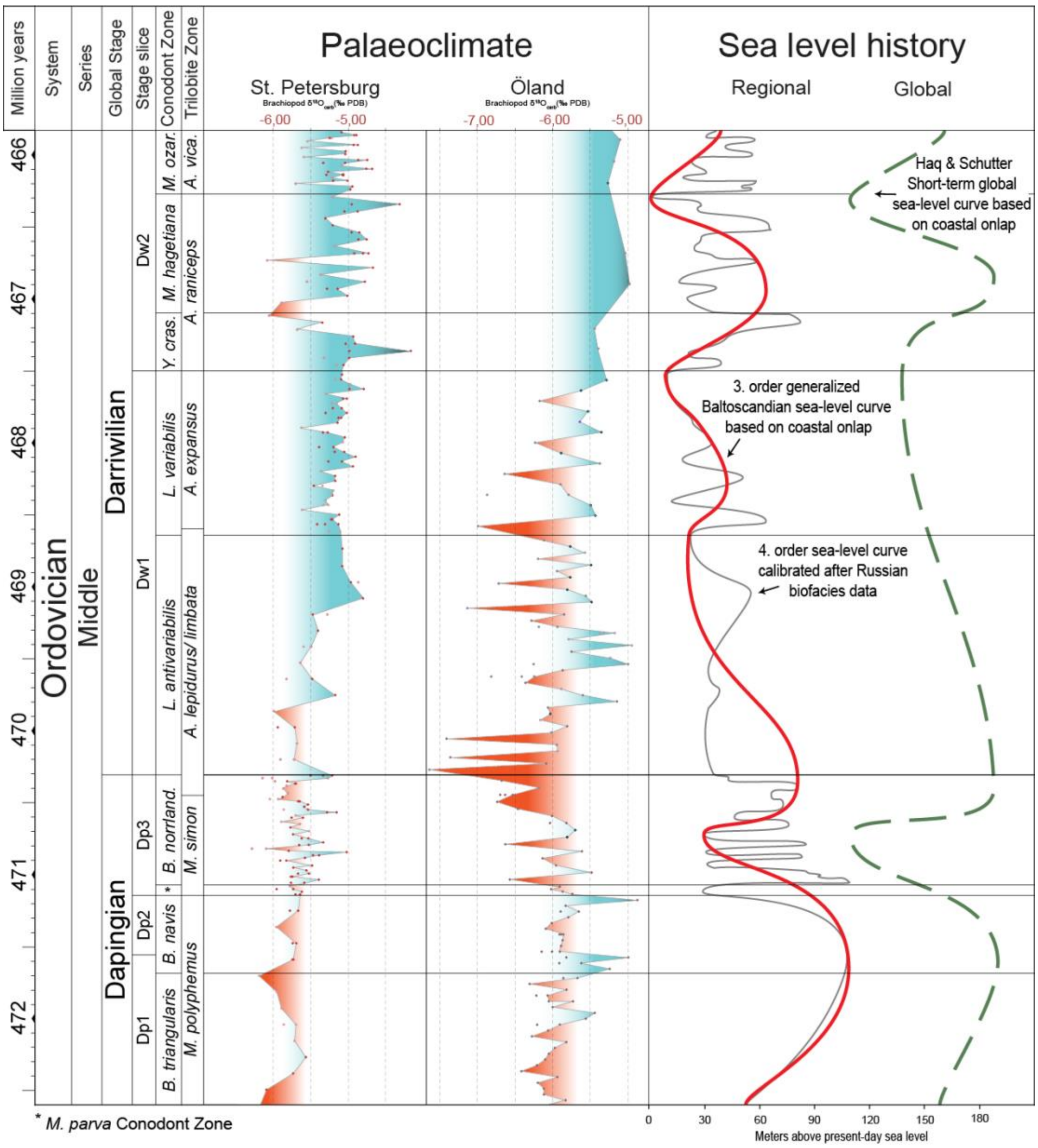

Figure 13: *Middle Ordovician $\delta^{18}O_{brachiopod}$ and sea level evolution across the Baltoscandian Paleobasin. Note that even though the 4th-order sea level curve (right) is based on a biofacies framework from the St. Petersburg region, individual excursions in the $\delta^{18}O$-Öland curve is still mirrored. $\delta^{18}O$-St. Petersburg curve and sea level curves as in C. M. Ø. Rasmussen et al.*

(2016) but here calibrated to the time domain. Original sea level data modified from Hansen & Nielsen (2003), Haq & Schutter (2008), A. T. Nielsen (1995, 2004, 2011); C. M. Ø. Rasmussen et al., 2009).

6.4.2 Deciphering orders of sea level change

In successions lacking a properly calibrated astrochronological framework – something still in its infancy when it comes to early Paleozoic rocks – only a high-resolution sequence- or ecostratigraphical analysis can resolve sea level changes at a sufficient temporal resolution to recognize glacio-eustasy. This has been done, in detail, on lowermost Darriwilian rocks of Baltica (A. T. Nielsen, 1995; C. M. Ø. Rasmussen et al., 2009, 2016) and Armorica (Dabard et al., 2015), revealing similar magnitude 3rd order sea level oscillations potentially at the kyr-scale. This interval precisely correlates to the interval where the current Baltic $\delta^{18}O$ record shows the strongest positive trend, in accordance with the inferred early Middle Ordovician sea level drop (Figure 13).
The trend towards relatively heavier late Darriwilian–Sandbian brachiopod $\delta^{18}O$ values reported here occurs at the start of an interval where global and regional sea level estimates suggest the start of a sea level rise that eventually peaked during the early–mid Katian (Hallam, 1992; Haq & Schutter, 2008; A. T. Nielsen, 2004; C. M. Ø. Rasmussen et al., 2019). This therefore seems to oppose a climatic driver for the oxygen isotope trend in this interval. However, as with the early Darriwilian (where there is a discordance between the actual brachiopod $\delta^{18}O$ trend and the expected trend based on the paleolatitudinal location of Baltica), there is a discordance between the $\delta^{18}O$-signal and inferred eustatic sea level rise during the later Darriwilian–Sandbian times as the latter would suggest a warming pulse. It is therefore expedient to distinguish between 1st-order plate tectonic-induced changes and the dramatic amplitudes of 4th and 3rd-order sea level changes suggestive of the waxing and waning of ice sheets (Hallam, 1992; Haq and Schutter, 2008; Nielsen, 2004; 2011). Whereas climatic cooling likely accelerated faster than the expected latitudinal temperature gradient during the early Darriwilian, the 1st-order sea level rise subsequently outpaced the 3rd-order sea level fall from the later Darriwilian onwards.

7 Conclusions

This study presents biostratigraphically well-resolved brachiopod and bulk carbonate carbon and oxygen isotope data spanning the Early (Floian) to early Late Ordovician (Sandbian) from Baltoscandia. The temporal scale of this Baltoscandian dataset allows for considerable refinement from a mid-latitude perspective of previously published global carbon and oxygen isotope data, which historically have been characterized by spot sampling across several paleoplates in low-latitude settings.

Several lines of evidence indicate that, while the carbon and oxygen isotope dataset may have been affected by diagenetic alteration, long-term trends in isotopic compositions which are useful for paleoenvironmental interpretation, are preserved. Our $\delta^{18}O$ record from Öland reveals that previously reported Early to Middle Ordovician $\delta^{18}O$ trends from eastern Baltoscandia are spatially consistent and together, the composite Baltoscandian $\delta^{18}O$ record is concordant with global Ordovician $\delta^{18}O$ compilations, which intimate an Early to Late Ordovician $\delta^{18}O$ increasing trend. We interpret the Baltoscandian $\delta^{18}O$ record as being dominated by a paleotemperature signal indicating a transition from warmer paleotemperatures during the Early Ordovician to cooler conditions in the Middle Ordovician.

Thus, the Baltoscandian $\delta^{18}O$ record is compatible with previous studies which suggest that present-day seawater temperatures were attained during the Darriwilian. This optimal temperature window may have sparked the GOBE.

Acknowledgements, Samples, and Data

We acknowledge Bo Petersen for help with isotope analysis, Laurent Nicod and Claudia Baumgartner (UNIL) for help with thin-section preparation. Morten L. Nielsen, Bristol, is thanked for field assistance, as are Cementa, the company operating the Degerhamn quarry, who permitted us to collect samples. The study was funded by a GeoCenter Denmark grant nos. 2015-5 and 3-2017 to CMØR. This paper is a contribution to IGCP project 653 – 'The onset of the Great Ordovician Biodiversification Event.' All datasets associated with the current study can be found at xx [to be uploaded upon acceptance of manuscript].

References

Ainsaar, L., Kaljo, D., Martma, T., Meidla, T., Männik, P., Nõlvak, J., & Tinn, O. (2010). Middle and Upper Ordovician carbon isotope chemostratigraphy in Baltoscandia: a correlation standard and clues to environmental histor. *Palaeogeography, Palaeoclimatology, Palaeoecology, 294*(3–4), 189–201.

Ainsaar, L., Meidla, T., & Tinn, O. (2004). *Middle and Upper Ordovician stable isotope stratigraphy across the facies belts in the East Baltic.* Paper presented at the Proceedings WOGOGOB-2004 Conference Materials, Tartu, 2004.

Ainsaar, L., Tinn, O., Dronov, A. V., Kiipli, E., & Radzevicius, S. (2020). Stratigraphy and facies differences of the Middle Darriwilian Isotopic Carbon Excursion (MDICE) in Baltoscandia. *Estonian Journal of Earth Sciences, 69*(4), 214–222. doi:https://doi.org/10.3176/earth.2020.16

Bagnoli, G., & Stouge, S. (1996). Changes in conodont provincialism and biofacies during the lower Ordovician in Öland, Sweden. *Palaeopelagoes, 6,* 19–29.

Bagnoli, G., & Stouge, S. (1997). Lower Ordovician (Billingenian–Kunda) conodont zonation and provinces based on sections from Horns Udde, north Öland, Sweden. *Bolletino della Società Paleontologica Italiana, 35,* 109–163.

Bagnoli, G., & Stouge, S. (1999). Bentonite beds and discontinuity surfaces as correlative tools in the Lower Ordovician carbonates of Baltoscandia. In A. Farinacci & A. R. Lord (Eds.), *Depositional Episodes and Bioevents* (pp. 29–38).

Barnes, C. R. (2004). Ordovician oceans and climate: The Great Ordovician Biodiversification Event. In (pp. 72–76).

Bergmann, K. D., Finnegan, S., Creel, R., Eiler, J. M., Hughes, N. C., Popov, L. E., & Fischer, W. W. (2018). A paired apatite and calcite clumped isotope thermometry approach to estimating Cambro–Ordovician seawater temperatures and isotopic composition. *Geochimica et Cosmochimica Acta, 224*, 18–41.

Bergström, S. M. (1971). Conodont biostratigraphy of the Middle and Upper Ordovician of Europe and eastern North America. *Geological Society of America Memoir, 127*, 83–161.

Bergström, S. M. (1980). Conodonts as paleotemperature tools in Ordovician rocks of the Caledonides and adjacent areas in Scandinavia and the British Isles. *Geologiska Föreningens i Stockholm Förhandlingar, 102*(4), 377–392.

Bergström, S. M. (2007). *The Ordovician conodont biostratigraphy in the Siljan region, south-central Sweden: a brief review of an international reference standard.* Paper presented at the 9th meeting of the Working Group on Ordovician Geology of Baltoscandia (WOGOGOB), Field Guide and Abstracts.

Bergström, S. M., Chen, X., Gutiérrez-Marco, J. C., & Dronov, A. (2009). The new chronostratigraphic classification of the Ordovician System and its relations to major regional series and stages and to $\delta^{13}C$ chemostratigraphy. *Lethaia, 42*, 97–107.

Bergström, S. M., Saltzman, M. R., Leslie, S. A., Ferretti, A., & Young, S. A. (2015). Trans-Atlantic application of the Baltic Middle and Upper Ordovician carbon isotope zonation. *Estonian Journal of Earth Sciences, 64*(1), 8-12. doi:doi: 10.3176/earth.2015.02

Bohlin, B. (1949). The Asaphus Limestone of Northernmost Öland. *Bulletin of the Geological Institutions of the University of Uppsala, 33*, 529–570.

Bohlin, B. (1953). The Lower Ordovician Limestone between the Ceratopyge Shale and the Platyurus Limestone of Böda Hamn. *Bulletin of the Geological Institution of the University of Upsala, 35*, 111–151.

Brand, U. (2004). Carbon, oxygen and strontium isotopes in Paleozoic carbonate components: an evaluation of original seawater-chemistry proxies. *Chemical Geology, 204*(1), 23–44.

Brand, U., Logan, A., Hiller, N., & Richardson, J. (2003). Geochemistry of modern brachiopods: applications and implications for oceanography and paleoceanography. *Chemical Geology, 198*, 305–334.

Brand, U., & Veizer, J. (1980). Chemical diagenesis of a multicomponent carbonate system; 1, Trace elements. *Journal of Sedimentary Research*, *50*(4), 1219–1236.

Brand, U., & Veizer, J. (1981). Chemical diagenesis of a multicomponent carbonate system – 2: stable isotopes. *Journal of Sedimentary Petrology, 51*(3), 987–997.

Bruckschen, P., & Veizer, J. (1997). Oxygen and carbon isotopic composition of Dinantian brachiopods: Paleoenvironmental implications for the Lower Carboniferous of western Europe. *Palaeogeography, Palaeoclimatology, Palaeoecology, 132*(1–4), 243–264.

Calner, M., Lehnert, O., Rongchang, W., Dahlqvist, P., & Joachimski, M. M. (2014). δ13C chemostratigraphy in Lower-Middle Ordovician succession of Öland (Sweden) and the global significance of the MDICE. *GFF, 136*(1), 48–54. doi:10.1080/11035897.2014.901409

Cárdenas, A. L., & Harries, P. J. (2010). Effect of nutrient availability on marine origination rates throughout the Phanerozoic eon. *Nature Geoscience*, *3*(6), 430-434.

Carpenter, S. J., & Lohmann, K. C. (1995). □18O and □13C values of modern brachiopod shells. *Geochimica et Cosmochimica Acta, 59*, 3749–3764.

Chen, J., & Lindström, M. (1991). Cephalopod septal strength indices (SSI) and depositional depth of Swedish Orthoceratite limestone. *Geologica et Paleontologica*, *25*, 5–18.

Cherns, L., Wheeley, J. R., Popov, L., Pour, M. G., Owens, R., & Hemsley, A. R. (2013). Long-period orbital climate forcing in the early Palaeozoic? *Journal of the Geological Society*, *170*(5), 707-710.

Cocks, L. R. M., & Torsvik, T. H. (2005). Baltica from the late Precambrian to the mid-Palaeozoic times: The gain and loss of a terrane's identity. *Earth-Science Reviews, 72*, 39-66.

Dabard, M. P., Loi, A., Paris, F., Ghienne, J. F., Pistis, M., & Vidal, M. (2015). Sea-level curve for the Middle to early Late Ordovician in the Armorican Massif (western France): Icehouse third-order glacio-eustatic cycles. *Palaeogeography Palaeoclimatology Palaeoecology, 436*, 96–111.

Edwards, C. T., Saltzman, M. R., Royer, D., & Fike, D. A. (2017). Oxygenation as a driver of the Great Ordovician Biodiversification Event. *Nature Geoscience*. doi:10.1038/s41561-017-0006-3

Egerquist, E. (2004). *Ordovician (Billingen and Volkhov stages) brachiopod faunas of the East Baltic.* (PhD). Uppsala University, Uppsala.

Ekdale, A. A., & Bromley, R. G. (2001). Bioerosional innovation for living in carbonate hardgrounds in the Early Ordovician of Sweden. *Lethaia, 34*(1), 1–12.

Eriksson, M. E., Lindskog, A., Calner, M., Mellgren, J. I. S., Bergström, S. M., Terfelt, F., & Schmitz, B. (2012). Biotic dynamics and carbonate microfacies of the conspicuous Darriwilian (Middle Ordovician) 'Täljsten' interval, south-central Sweden. *Palaeogeography, Palaeoclimatology, Palaeoecology, 367–368*, 89–103.

Fang, Q., Wu, H., Wang, X., Yang, T., Li, H., & Zhang, S. (2019). An astronomically forced cooling event during the Middle Ordovician. *Global and Planetary Change, 173,* 96-108.

Finnegan, S., Bergmann, K., Eiler, J. M., Jones, D. S., Fike, D. A., Eisenman, I., . . . Fischer, W. W. (2011). The Magnitude and Duration of Late Ordovician–Early Silurian Glaciation. *Science, 331,* 903-906.

Fortey, R. A., & Cocks, L. R. M. (2005). Late Ordovician global warming - The Boda Event. *Geology, 33,* 405-408.

Ghobadi Pour, M., Williams, M., & Popov, L. E. (2007). A new Middle Ordovician arthropod fauna (Trilobita, Ostracoda, Bradoriida) from the Lashkarak Formation, Eastern Alborz Mountains, northern Iran. *GFF, 129*, 245–254.

Goldberg, S. L., Present, T. M., Finnegan, S., & Bergmann, K. D. (2021). A high-resolution record of early Paleozoic climate. *Proceedings of the National Academy of Sciences, 118*(6).

Gradstein, F., & Ogg, J. (2020). The chronostratigraphic scale. In *Geologic Time Scale 2020* (pp. 21-32): Elsevier.

Hallam, A. (1992). *Phanerozoic sea-level changes*. New York: Columbia University Press.

Hansen, T., & Nielsen, A. T. (2003). Upper Arenig trilobite biostratigraphy and sea-level changes at Lynna River near Volkhov, Russia. *Bulletin of the Geological Society of Denmark, 50*, 105-114.

Haq, B. U., & Schutter, S. R. (2008). A chronology of Paleozoic sea-level changes. *Science, 322,* 64–68.

Huff, W. D., Bergström, S. M., & Kolata, D. R. (1992). Gigantic Ordovician volcanic ash fall in North America and Europe: Biological, tectonomagmatic, and event-stratigraphic significance. *Geology, 20*(10), 875–878.

Jaffrés, J. B., Shields, G. A., & Wallmann, K. (2007). The oxygen isotope evolution of seawater: A critical review of a long-standing controversy and an improved geological water cycle model for the past 3.4 billion years. *Earth-Science Reviews, 83*(1–2), 83–122.

Jaanusson, V. (1960). The Viruan (Middle Ordovician) of Öland. *Bulletin of the Geological Institutions of the University of Uppsala, 38*, 207–288.

Jaanusson, V. (1961). Discontinuity surfaces in limestones. *Bulletin of the Geological Institutions of the University of Uppsala, 40*(35), 221–241.

Jaanusson, V. (1976). Faunal dynamics in the Middle Ordovician (Viruan) of Balto-Scandia. In M. G. Bassett (Ed.), *The Ordovician System, Proceedings of a Palaeontological Association Symposium, Birmingham 1974* (pp. 301–326.). Cardiff: University of Wales Press and National Museums of Wales.

Jaanusson, V. (1982a). *Introduction to the Ordovician of Sweden*. Paper presented at the 4th International Symposium on the Ordovician System, Oslo.

Jaanusson, V. (1982b). *Ordovician in Västergötland.* Paper presented at the Field Excursion Guide. 4th International Symposium on the Ordovician System.

Jaanusson, V. (1995). Confacies differentiation and upper Middle Ordovician correlation in the Baltoscandian Basin. *Proceedings of the Estonian Academy of Sciences, Geology, 44*(2), 73–86.

Kaljo, D., Martma, T., & Saadre, T. (2007). Post-Hunnebergian Ordovician carbon isotope trend in Baltoscandia, its environmental implications and some similarities with that of Nevada. *Palaeogeography, Palaeoclimatology, Palaeoecology, 245*(1–2), 138–155.

Knoll, A. H., & Carroll, S. B. (1999). Early animal evolution: emerging views from comparative biology and geology. *Science, 284*(5423), 2129-2137.

Korte, C., & Hesselbo, S. P. (2011). Shallow marine carbon and oxygen isotope and elemental records indicate icehouse-greenhouse cycles during the Early Jurassic. *Paleoceanography, 26*(4), 18 pp. doi: https://doi.org/10.1029/2011PA002160

Korte, C., Jones, P. J., Brand, U., Mertmann, D., & Veizer, J. (2008). Oxygen isotope values from high-latitudes: Clues for Permian sea-surface temperature gradients and Late Palaeozoic deglaciation. *Palaeogeography, Palaeoclimatology, Palaeoecology, 269*, 1–16. doi:doi:10.1016/j.palaeo.2008.06.012.

Kroopnick, P., Margolis, S., & Wong, C. (1977). Paleoproductivity and ΣCO2-13C correlations in the atmosphere and oceans. The Fate of Fossil Fuel Carbonates. *Office of Naval Research Symposium Series in Oceanography*.

Kröger, B., Franeck, F., & Rasmussen, C. M. Ø. (2019). The evolutionary dynamics of the early Palaeozoic marine biodiversity accumulation. *Proceedings of the Royal Society B, 286*, 20191634.

Le Hérissé, A., Al-Ruwaili, M., Miller, M., & Vecoli, M. (2007). Environmental changes reflected by palynomorphsintheearlyMiddleOrdovicianHanadir Member of the Qasim Formation, Saudi Arabia. *Revue de micropaleontology, 50*, 3–16.

Lehnert, O., Meinhold, G., Wu, R.-C., Calner, M., & Joachimski, M. M. (2014). δ13C chemostratigraphy in the upper Tremadocian through lower Katian (Ordovician) carbonate succession of the Siljan district, central Sweden. *Estonian Journal of Earth Sciences, 63*(4), 277– 286.

Lindskog, A., Costa, M. M., Rasmussen, C. M. Ø., Connelly, J. N., & Eriksson, M. E. (2017). Refined Ordovician timescale reveals no link between asteroid breakup and biodiversification. *Nature Communications, 8*, 14066. doi:10.1038/ncomms14066

Lindskog, A., & Eriksson, M. E. (2017). Megascopic processes reflected in the microscopic realm: sedimentary and biotic dynamics of the Middle Ordovician “orthoceratite limestone” at Kinnekulle, Sweden. *GFF, 139*(3), 163–183.

Lindskog, A., Eriksson, M. E., Bergström, S. M., & Young, S. A. (2019). Lower–Middle Ordovician carbon and oxygen isotope chemostratigraphy at Hällekis, Sweden: implications for regional to global correlation and paleoenvironmental development. *Lethaia, 52*(2), 204–219.

Lindström, M. (1963). Sedimentary folds and the development of limestone in the early Ordovician sea. *Sedimentology, 2*, 243–292.

Lindström, M. (1971). Lower Ordovician conodonts of Europe. *Geological Society of America Memoir, 127*, 21–61.

Lindström, M. (1979). Diagenesis of Lower Ordovician hardgrounds in Sweden. *Geologica et palaeontologica, 13*, 9–30.

Lindström, M. (1984). The Ordovican climate based on the study of carbonate rocks. In D. L. Bruton (Ed.), *Aspects of the Ordovician System* (Vol. 295, pp. 81–88): Universitetforlaget.

Löfgren, A. (2000). Early to early Middle Ordovician conodont biostratigraphy of the Gillberga quarry, northern Öland, Sweden. *GFF, 122*(4), 321–338.

Löfgren, A. (2003). Conodont faunas with Lenodus variabilis in the upper Arenigian to lower Llanvirnian of Sweden. *Acta Palaeontologica Polonica, 48*(3), 417–436.

McKenzie, N. R., Hughes, N. C., Gill, B. C., & Myrow, P. M. (2014). Plate tectonic influences on Neoproterozoic–early Paleozoic climate and animal evolution. *Geology, 42*(2), 127–130. doi:10.1130/G34962.1

Miller, A. I., & Mao, S. (1995). Association of orogenic activity with the Ordovician radiation of marine life. *Geology, 23*(4), 305-308.

Munnecke, A., Calner, M., Harper, D. A. T., & Servais, T. (2010). Ordovician and Silurian sea-water chemistry, sea-level, and climate: a synopsis. *Palaeogeography, Palaeoclimatology, Palaeoecology, 296*, 389-413.

Männil, R. (1966). *Evolution of the Baltic Basin during the Ordovician*. Tallinn: Valgus Publishers.

Nielsen, A. T. (1995). Trilobite systematics, biostratigraphy and palaeoecology of the Lower Ordovician Komstad Limestone and Huk Formations, Southern Scandinavia. *Fossils and Strata, 38*, 1-374.

Nielsen, A. T. (2004). Ordovician Sea Level Changes: A Baltoscandian Perspective. In B. D. Webby, F. Paris, M. L. Droser, & I. C. Percival (Eds.), *The Great Ordovician Biodiversification Event* (pp. 84 - 93). New York: Columbia University Press.

Nielsen, A. T. (2011). A re-calibrated revised sea-level curve for the Ordovician of Baltoscandia. *Cuadernos del Museo Geominero, 14*, 399-401.

Qing, H., & Veizer, J. (1994). Oxygen and carbon isotopic composition of Ordovician brachiopods: Implications for coeval seawater. *Geochimica et Cosmochimica Acta, 58*(20), 4429–4442.

Quinton, P. C., Speir, L., Miller, J., Ethington, R., & MacLeod, K. G. (2018). extreme heat in the Early Ordovician. *Palaios, 33*, 353–360. doi:http://dx.doi.org/10.2110/palo.2018.031

Rasmussen, B. W., Rasmussen, J. A., & Nielsen, A. T. (2017). Biostratigraphy of the Furongian (upper Cambrian) Alum Shale Formation at Degerhamn, Öland, Sweden. *GFF, 139*(2), 92–118.

Rasmussen, C. M. Ø., Kröger, B., Nielsen, M. L., & Colmenar, J. (2019). Cascading trend of early Paleozoic marine radiations paused by Late Ordovician mass extinctions. *PNAS, 116*(15), 7207–7213. doi:10.1073/pnas.1821123116

Rasmussen, C. M. Ø., Nielsen, A. T., & Harper, D. A. T. (2009). Ecostratigraphical interpretation of lower Middle Ordovician East Baltic sections based on brachiopods. *Geological Magazine, 146*(5), 717-731. doi:10.1017/s0016756809990148

Rasmussen, C. M. Ø., Ullmann, C. V., Jakobsen, K. G., Lindskog, A., Hansen, J., Hansen, T., . . . Harper, D. A. T. (2016). Onset of main Phanerozoic marine radiation sparked by emerging Mid Ordovician icehouse. *Scientific Reports, 6*, 18884. doi:DOI: 10.1038/srep18884

Rasmussen, J. A., & Stouge, S. (2018). Baltoscandian conodont biofacies fluctuations and their link to middle Ordovician (Darriwilian) global cooling. *Palaeontology, 61*, 391–416.

Saltzman, M. M., & Thomas, E. (2012). Cahapter 11 – carbon isotope stratigraphy. In F. M. Gradstein, J. G. Ogg, M. Schmitz, & G. Ogg (Eds.), *The Geologic Time Scale 2012* (pp. 207–232). Amsterdam: Elsevier BV.

Saltzman, M. R., & Edwards, C. T. (2017). Gradients in the carbon isotopic composition of Ordovician shallow water carbonates: A potential pitfall in estimates of ancient CO2 and O2. *Earth and Planetary Science Letters, 464*, 46–54. doi:10.1016/j.epsl.2017.02.011

Saltzman, M. R., & Young, S. A. (2005). Long-lived glaciation in the Late Ordovician? Isotopic and sequence-stratigraphic evidence from western Laurentia. *Geology, 33*, 109-112.

Schmitz, B., Bergström, S. M., & Xiaofeng, W. (2010). The middle Darriwilian (Ordovician) ^{13}C excursion (MDICE) discovered in the Yangtze Platform succession in China: implications of its first recorded occurrences outside Baltoscandia. *Journal of Geological Society (London), 167*, 249-259.

Schmitz, B., Farley, K. A., Goderis, S., Heck, P. R., Bergström, S. M., Boschi, S., . . . Terfelt, F. (2019). An extraterrestrial trigger for the mid-Ordovician ice age: Dust from the breakup of the L-chondrite parent body. *Science Advances, 5*(eaax4184).

Schobben, M., Ullmann, C. V., Leda, L., Korn, D., Struck, U., Reimold, W. U., . . . Korte, C. (2016). Discerning primary versus diagenetic signals in carbonate carbon and oxygen isotope records: An example from the Permian–Triassic boundary of Iran. *Chemical Geology, 422*, 94–107.

Shields, G. A., Carden, G. A. F., Veizer, J., Meidla, T., Rong, J.-y., & Li, R.-y. (2003). Sr, C, and O isotope geochemistry of Ordovician brachiopods: A major isotopic event around the Middle-Late Ordovician transition. *Geochimica et Cosmochimica Acta, 67*(11), 2005–2025.

Steuber, T., & Veizer, J. (2002). Phanerozoic record of plate tectonic control of seawater chemistry and carbonate sedimentation. *Geology, 30*(12), 1223–1126.

Stouge, S. (2004). *Ordovician siliciclastics and carbonates of Öland, Sweden, 91–111*. Paper presented at the Annual Meeting of IGCP Project No 503, Erlangen, Germany.

Stouge, S., & Bagnoli, G. (1990). Lower Ordovician (Volkhovian–Kundan) conodonts from Hagudden, northern Öland, Sweden. *Paleontographia Italica, 77*, 1–54.

Stouge, S., & Bagnoli, G. (2014). *Timing of the deposition of the remarkable 'green unit' (early Middle Ordovician) on Öland, Sweden*. Paper presented at the 4th Annual Meeting of IGCP 591 – Abstracts and Field Guide Tartu, Estonia.

Stouge, S., Bagnoli, G., & Rasmussen, J. A. (2020). Late Cambrian (Furongian) to mid-Ordovician euconodont events on Baltica: Invasions and immigrations. *Palaegeography, Palaeoclimatology, Palaeoecology, In press*. doi:doi.org/10.1016/j.palaeo.2019.04.007

Swart, P. K. J. S. (2015). The geochemistry of carbonate diagenesis. *The past, present and future, 62*(5), 1233–1304.

Terfelt, F., Eriksson, M. E., & Schmitz, B. (2014). The Cambrian–Ordovician transition in dysoxic facies in Baltica—diverse faunas and carbon isotope anomalies. *Palaeogeography, Palaeoclimatology, Palaeoecology, 394*, 59–73.

Torsvik, T. H., & Cocks, L. R. M. (2016). Ordovician. In *Earth history and paleogeography* (pp. 101–123): Cambridge University Press.

Torsvik, T. H., & Rehnström, E. (2003). The Tornquist Sea and Baltica – Avalonia docking. *Tectonophysics, 362*, 67-82.

Torsvik, T. H., Smethurst, M. A., Voo, R. V. D., Trench, A., Abrahamsen, N., & Halvorsen, E. (1992). Baltica. A synopsis of Vendian – Permian palaeomagnetic data and their palaeotectonic implications. *Earth-Science Reviews, 33*, 133-152.

Torsvik, T. H., Van der Voo, R., Preeden, U., MacNiocaill, C., Steinberger, B., Doubrovine, P. V., . . . Cocks, L. R. M. (2012). Phanerozoic polar wander, palaeogeography and dynamics. *Earth-Science Reviews, 114*(325-368).

Trotter, J. A., Williams, I. S., Barnes, C. R., Lécuyer, C., & Nicoll, R. S. (2008). Did cooling oceans trigger Ordovician biodiversification? Evidence from conodonts thermometry. *Science, 321*, 550-554.

Tullborg, E.-L., Larsson, S. A., Björklund, L., Stigh, J., & Samuelsson, L. (1995). Thermal evidence of Caledonide foreland, molasse sedimentation in Fennoscandia. *Swedish Nuclear Fuel and Waste Management Company Technical Report, 95–18,* 47 pp.

Turner, B. R., Armstrong, H. A., Wilson, C. R., & Makhlouf, I. M. (2012). High frequency eustatic sea-level changes during the Middle to early Late Ordovician of southern Jordan: Indirect evidence for a Darriwilian Ice Age in Gondwana. *Sedimentary Geology, 251–252*, 34–48.

Ullmann, C. V., & Korte, C. (2015). Diagenetic alteration in low-Mg calcite from macrofossils: a review. *Geological Quarterly, 59*(1), 3–20. doi:10.7306/gq.1217

Ullmann, C., Frei, R., Korte, C., & Lüter, C. (2017). Element/Ca, C and O isotope ratios in modern brachiopods: Species-specific signals of biomineralization. *Chemical Geology, 460*, 15–24.

Ullmann, C. V., Campbell, H. J., Frei, R., Hesselbo, S. P., Pogge von Strandmann, P. A. E., & Korte, C. (2013). Partial diagenetic overprint of Late Jurassic belemnites from New Zealand: implications for the preservation of δ^7Li values in calcite fossils. *Geochimica et Cosmochimica Acta, 120*, 80–96.

Valentine, J. W., & Moores, E. W. (1970). Plate-tectonic regulation of faunal diversity and sea level: a model. *Nature, 228*, 657–659.

van de Schootbrugge, B., Föllmi, K. B., Bulot, L. G., & Burns, S. J. (2000). Paleoceanographic changes during the early Cretaceous (Valanginian–Hauterivian): evidence from oxygen and carbon stable isotopes. *Earth and Planetary Science Letters, 181*(1–2), 15–31.

van Wamel, W. A. (1974). Conodont biostratigraphy of the Upper Cambrian and Lower Ordovician of north-western Öland, south-eastern Sweden. *Utrecht micropaleontological bulletins, 10*.

Vandenbroucke, T. R. A., Armstrong, H. A., Williams, M., Paris, F., Zalasiewicz, J., Sabbe, K., . . . Servais, T. (2010). Polar front shift and atmospheric CO_2 during the glacial maximum of the Early Paleozoic Icehouse. *PNAS, 107*(34), 14983–14986. doi:10.1073/pnas.1003220107

Veizer, J., Ala, D., Azmy, K., Bruckschen, P., Buhl, D., Bruhn, F., . . . Godderis, Y. (1999). 87Sr/86Sr, δ13C and δ18O evolution of Phanerozoic seawater. *Chemical Geology, 161*, 92–104.

Veizer, J., Godderis, Y., & Francois, L. M. (2000). Evidence for decoupling of atmospheric CO2 and global climate during the Phanerozoic eon. *Nature*, *408*, 698-701.

Veizer, J., & Prokoph, A. (2015). Temperatures and oxygen isotopic composition of Phanerozoic oceans. *Earth-Science Reviews*, *146*, 92–104.

Wu, R., Calner, M., & Lehnert, O. (2017). Integrated conodont biostratigraphy and carbon isotope chemostratigraphy in the Lower–Middle Ordovician of southern Sweden reveals a complete record of the MDICE. *Geological Magazine, 154*(2), 334-353.

Young, S. A., Gill, B. C., Edwards, C. T., Saltzman, M. R., & Leslie, S. A. (2016). Middle–Late Ordovician (Darriwilian–Sandbian) decoupling of global sulfur and carbon cycles: Isotopic evidence from eastern and southern Laurentia. *Palaeogeography, Palaeoclimatology, Palaeoecology, 458*, 118–132. doi:https://doi.org/10.1016/j.palaeo.2015.09.040

Zaffos, A., Finnegan, S., & Peters, S. E. (2017). Plate tectonic regulation of global marine animal diversity. *Proceedings of the National Academy of Sciences, 114*(22), 5653-5658.

Zhan, R., Jin, J., & Chen, P. (2007). Brachiopod diversification during the Early-Mid Ordovician: an example from the Dawan Formation, Yichang area, central China. *Canadian Journal of Earth Sciences, 44*(1), 9–24.

Zhang, J. (1998). Middle Ordovician conodonts from the Atlantic Faunal Region and the evolution of key conodont genera. *Meddelanden från Stockholms universitets institution för geologi och geokem, 298*, 1101–1599.